Long-term changes on the Bransfield Strait deep water masses: Variability, drivers and connections with the northwestern Weddell Sea

Brendon Yuri Damini, Rodrigo Kerr, Tiago S. Dotto, Mauricio M. Mata

PII: S0967-0637(21)00204-1

DOI: https://doi.org/10.1016/j.dsr.2021.103667

Reference: DSRI 103667

To appear in: *Deep-Sea Research Part I*

Received Date: 14 April 2021

Revised Date: 24 October 2021

Accepted Date: 5 November 2021

Please cite this article as: Damini, B.Y., Kerr, R., Dotto, T.S., Mata, M.M., Long-term changes on the Bransfield Strait deep water masses: Variability, drivers and connections with the northwestern Weddell Sea, *Deep-Sea Research Part I* (2021), doi: https://doi.org/10.1016/j.dsr.2021.103667.

Long-term changes on the Bransfield Strait deep water masses: variability, drivers and connections with the northwestern Weddell Sea

Brendon Yuri Damini[1,2,*], Rodrigo Kerr[1,2,*], Tiago S. Dotto[1,3], and Mauricio M. Mata[1,2]

[1]Laboratório de Estudos dos Oceanos e Clima, Instituto de Oceanografia, Universidade Federal do Rio Grande – FURG, Av. Itália km 8 s/n, Rio Grande, RS, 96203–900, Brazil.

[2]Programa de Pós-Graduação em Oceanologia, Instituto de Oceanografia, Universidade Federal do Rio Grande – FURG, Av. Itália km 8 s/n, Rio Grande, RS, 96203–900, Brazil.

[3]Now at: Centre for Ocean and Atmospheric Sciences, School of Environmental Sciences, University of East Anglia, Norwich, NR4 7TJ, UK.

*Corresponding authors:

Address: CEOCEAN, Instituto de Oceanografia, Universidade Federal do Rio Grande – FURG, Av. Itália km8 s/n, Rio Grande, RS, 96203–900, Brazil.

E–mails: Brendon Damini (brendon.oceano@furg.br), Rodrigo Kerr (rodrigokerr@furg.br)

Highlights:

- Long–term cooling, freshening, and lightening (1963-2019) of deep waters in the Bransfield central basin.
- Decreasing ventilation in the Bransfield Strait eastern basin as oxygen declined.
- Reversal of freshening trend between 2010 and 2016 associated with increased contribution of High Salinity Shelf Water.
- Decreasing in salinity after 2016 caused by increased contribution of Low Salinity Shelf Water.
- Increased contribution of High Salinity Shelf Water in the Bransfield Strait related to increased sea ice cover in the northwestern Weddell Sea.

Submitted to Deep Sea Research Part I: Oceanographic Research Papers

Abstract

The Bransfield Strait receives substantial input from recently ventilated Dense Shelf Water (i.e., High Salinity Shelf Water – HSSW or Low Salinity Shelf Water – LSSW) formed in the Weddell Sea continental shelf. The bathymetric restricted connections to the surrounding oceans make the Bransfield Strait's deep basins proxy regions to study the temporal variability of these waters. HSSW is an important precursor to Antarctic Bottom Water, a water mass with a global impact on the deeper branches of the global overturning circulation. The deep waters in the central basin of the Bransfield Strait have unveiled significant long–term cooling, freshening, and lightening between 1963 and 2019. Conversely, in the eastern basin of the Bransfield Strait, signals of freshening, lightening, and decreasing of dissolved oxygen have been present since 1975, but somewhat less robust than those founded on the central basin. Hence, that dichotomy in neighboring regions influenced by same source water masses suggests different mixing proportions and variability, likely resulting from distinct source regions of the dense waters precursors. In addition, the deep water masses in the Bransfield Strait have shown a strong interannual variability of thermohaline properties, which is mainly explained by the El Niño–Southern Oscillation and the Southern Annular Mode. These climate modes are likely to influence the periods of increasing salinity, such as 2010 to 2016, favoring higher intrusions of HSSW rather than the less dense variety into the Bransfield Strait. Evidence to the increased contribution of HSSW during that period may be explained by an increase in the sea ice formation in the Weddell Sea. During the sea ice formation, higher rates of Dense Shelf Water was likely formed in the northwestern Weddell Sea due to brine rejection. The changes reported here are key to add new insights on a better understanding of how changes in the source water masses can affect the deep branches of the global overturning circulation cell, which is still a challenging question for the community. Finally, the hydrographic properties time series in the Bransfield Strait used here spanned through six decades, which is much longer than those previously reported in the Weddell Sea, providing further and stronger evidence on how climate variability affects bottom water in the Southern Ocean.

Keywords: OMP analysis; Dense Shelf Water; climate modes; sea ice concentration; deep water masses; freshening; Southern Ocean.

1. Introduction

The Bransfield Strait is a semi–closed ocean basin located in the northern Antarctic Peninsula between latitudes 60º–64ºS and longitudes 53º–62ºW (Figure 1a; López et al., 1999; Kerr et al., 2018a). Morphologically, the Bransfield Strait has three deep basins (i.e., western, central, and eastern) separated by relatively shallow sills (Gordon & Nowlin, 1978) that retain a combination of varieties of the Circumpolar Deep Water (CDW; relatively warm, salty, deoxygenated, and carbon–rich) and quasi-pure cold and salty Dense Shelf Water varieties formed in the Weddell Sea (Gordon et al., 2000; Dotto et al., 2016). The Bransfield Strait central and eastern deep basins are filled with a mixture of the Dense Shelf Water varieties named Low Salinity Shelf Water (LSSW) and High Salinity Shelf Water (HSSW) that combined account for 90% and 65% of contribution in each basin, respectively (Wilson et al., 1999; Dotto et al., 2016). The remaining percentage is sourced by mixing of modified CDW (mCDW) and/or Warm Deep Water (i.e., the CDW variety observed in the Weddell Sea; Gordon et al., 2000). While mCDW enters the strait through the gaps between the South Shetlands Island (i.e., King George, Elephant, Snow, Smith and Low Islands) and the Antarctic Peninsula (Figure 1a; Niler et al., 1991; Hofmann et al., 1996), the Dense Shelf Water are advected into the Bransfield Strait by following the Antarctic Coastal Current and contouring the tip of the Antarctic Peninsula (von Gyldenfeldt et al., 2002; Heywood et al., 2004; Huneke et al., 2016; Sangrà et al., 2017; Collares et al., 2018; van Caspel et al., 2018). Once in the Bransfield Strait, these dense waters sink into the deep basins, a process facilitated by the several canyons existing on the continental shelf of the Antarctic Peninsula (López et al., 1999). The bathymetric constraints of the deep basins, especially the central basin, limit the mixing with the surrounding water masses, allowing conditions to preserve the thermohaline characteristics of these Dense Shelf Water (Wilson et al., 1999; Gordon et al., 2000; van Caspel et al., 2015; Dotto et al., 2016; van Caspel et al., 2018).

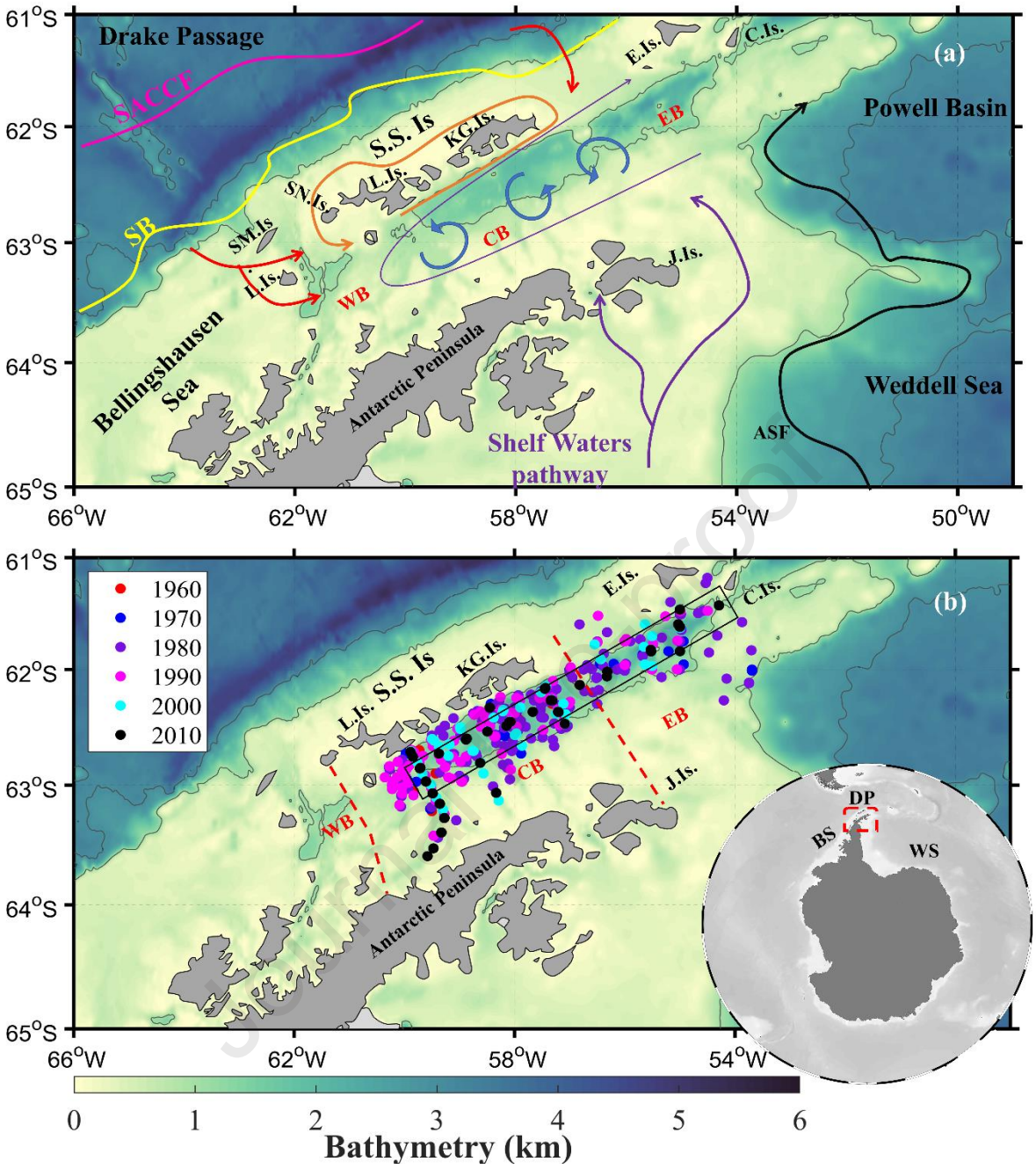

Figure 1. (a) Schematic representation of the circulation of the Bransfield Strait, following Garcia et al. (2002), Zhou et al. (2002), and Sangrà et al. (2017). The arrows represent the pathways of the Circumpolar Deep Water (red) and Dense Shelf Water (purple) entering the strait. The pink and yellow lines represent the mean locations of the Southern Antarctic Circumpolar Current Front (SACCF) and the Southern Boundary of the Antarctic Circumpolar Current (SB), respectively, following Orsi et al. (1995). The submesoscale eddies along the Bransfield Strait, are shown by light blue arrows. The black arrow represents the mean location of the Antarctic Slope Front (ASF; Heywood et al., 2004). The orange arrow depicts the recirculation around the South Shetland Islands (S.S.Is.). (b) Map of the hydrographic station's location in the Bransfield Strait for the period from the 1960s to 2010s. The colors represent the decades, according to the legend. The stations used were selected after the criteria of density ($\gamma^n \geq 28.27$ kg m^{-3}) and depths (> 800 m). The black rectangle represents the repetition line used in the Optimum Multiparameter analysis. The red dotted lines represent the limits of the basins (WB = western basin, CB = central basin, and EB = eastern basin) used in this work.

BS = Bellingshausen Sea, DP = Drake Passage, WS = Weddell Sea, WB = Western Basin, CB = Central Basin and EB = Eastern Basin, L. Is. = Livingston Island, K.G. Is. = King George Island, J. Is. = Joinville Island, E. Is = Elephant Island, C. Is. = Clarence Island, SM. Is = Smith Island, SN. Is = Snow Island.

Several studies have shown signals of freshening and lightening of the Bransfield Strait deep waters over the past 50 years (e.g., Wilson et al., 1999; Garcia & Mata, 2005; Azaneu et al., 2013; Dotto et al., 2016; Ruiz Barlett et al., 2018). For instance, Dotto et al. (2016) reported for the period spanning from 1963 to 2014 signs of freshening (with rates of $–0.0010 \pm 0.0005$ $yr^{–1}$ and $–0.0010 \pm 0.0006$ $yr^{–1}$) and lightening (with rates of $–0.0016 \pm 0.0014$ kg $m^{–3}$ $yr^{–1}$ and $–0.0029 \pm 0.0013$ kg $m^{–3}$ $yr^{–1}$) for the deepest and most stable layers of the central and eastern basins of the Bransfield Strait. These trends agree with a reported pan-Antarctic freshening of the shelf waters (Azaneu et al., 2013; Schmidtko et al., 2014). Given that the shelf waters are source for the Antarctic Bottom Water (AABW), this water mass has also been losing volume due to the formation of a less dense variety (Rintoul, 2007; Hellmer et al., 2011; Purkey & Johnson, 2012; Azaneu et al., 2013; Schmidtko et al., 2014; van Wijk & Rintoul, 2014; Lago & England, 2019; Aoki et al., 2020a). The freshening signals observed in the Bransfield Strait (Azaneu et al., 2013; Dotto et al., 2016; Ruiz Barlett et al., 2018) and in the Dense Shelf Water (Hellmer et al., 2011; Schmidko et al., 2014) might be associated with the melting of the ice shelves and glaciers around the western Weddell Sea (Paolo et al., 2015; Cook et al., 2016; Shepherd et al., 2018; Rignot et al., 2019), which injected ~24 Gt $yr^{–1}$ of freshwater into the system between 1979−2017 (Rignot et al., 2019). These long–term trends indicate the climatic vulnerability of the region and hence the need for further investigation (Moffat & Meredith et al., 2018; Kerr et al., 2018a; Henley et al., 2019).

Despite the long-term freshening, the water masses properties of the Bransfield Strait are also characterized by strong interannual variability. For instance, Dotto et al. (2016) reported increased salinity in the deep central and eastern basins after 2010, associated with

132 increased input of HSSW into the Bransfield Strait. The rise in salinity was strong enough to
133 bring the mean-salinity of 2014 (i.e., last year of their time series) close to the ones reported
134 for the early-1980s. These interannual changes in the hydrographic and also the
135 biogeochemical properties distribution may be recently linked with large-scale climate modes
136 of variability, such as the Southern Annular Mode (SAM) and the El Niño–Southern
137 Oscillation (ENSO) (e.g., Dotto et al., 2016; Ruiz Barlett et al., 2018; Avelina et al., 2020).

138 During the positive SAM phase (Figure S1a), stronger westerly winds shift the position
139 of the Southern Antarctic Circumpolar Current Front (SACCF) and the Southern Boundary of
140 Antarctic Circumpolar Current (SB; Figure 1a; Orsi et al., 1995) towards the Antarctic
141 Peninsula (Marshall et al., 2004; Renner et al., 2012). Simultaneously, both the circulation of
142 the Weddell Gyre and the flow of the Antarctic Slope Current are accelerated by the
143 strengthening of the negative wind stress curl upon the region, thus limiting the connection
144 between the Weddell Sea and the areas to the west of the Antarctic Peninsula (Renner et al.,
145 2012; Youngs et al., 2015). This configuration reduces transports of saltier and denser varieties
146 of Dense Shelf Water into the Bransfield Strait central and eastern basins (Dotto et al., 2016).
147 Conversely, during the negative SAM phase (Figure S1b), weaker westerly winds displace the
148 SACCF and SB further north, and the Weddell Gyre and Antarctic Slope Current are
149 decelerated by the weakening of the negative wind stress curl upon the region (Marshall et al.,
150 2004; Mckee et al., 2011; Renner et al., 2012). In addition, coastal currents on the western
151 Weddell Sea are intensified, enabling the transport of saltier and denser varieties of Dense Shelf
152 Water into the Bransfield Strait (Dotto et al., 2016; van Caspel et al., 2018).

153 ENSO affects the strength and frequency of northwesterly winds in the region (Yuan et
154 al., 2004). During the negative phases (La Niña; Figure S1c), the northwesterly winds are
155 strengthened and more frequent (Yuan, 2004), and thus the SACCF and SB shift towards the
156 Antarctic Peninsula, therefore moving more CDW into Bransfield Strait (Loeb et al., 2010;

157 Ruiz Barlett et al., 2018). Conversely, during the ENSO positive phase (El Niño; Figure S1d),
158 northerly winds are less frequent and weaker on the western Antarctic Peninsula.
159 Consequently, the SACCF and SB are displaced further north, and less CDW moves into the
160 Bransfield Strait (Ruiz Barlett et al., 2018). Moreover, when both modes are in phase, i.e.,
161 during La Niña and positive SAM (El Niño and negative SAM), the advection of CDW into
162 Bransfield Strait is increased (weakened), which is associated with the weakening (increasing)
163 of the transport of shelf waters along the west Antarctic Peninsula (Ruiz Barlett et al., 2018).

164 In this context, and after inferences from observation and modelling studies (Dotto et
165 al. 2016; van Caspel et al., 2018), this study aims to investigate the origin and variability of the
166 deep water masses in the Bransfield Strait basins, strengthening the current knowledge of the
167 ocean dynamics in a climate sensitive region of the Southern Ocean. Furthermore, the long–
168 term variability of the hydrographic properties of the Bransfield Strait was evaluated through
169 the hypothesis that the higher sea ice formation in the northwestern Weddell Sea, associated
170 with ENSO and SAM, increases the brine rejection over the continental shelf and caused an
171 increase in HSSW contribution in recent years.

172 **2. Data and Methods**

173 **2.1. Hydrographic Data**

174 We used historical data from (i) World Ocean Database 2013 (Boyer et al., 2013), (ii)
175 PANGAEA (https://www.pangaea.de/), and (iii) spatial high–resolution data acquired by the
176 Brazilian High Latitude Oceanography Group (GOAL; www.goal.furg.br; Mata et al., 2018).
177 Data from 1963 to 2019 were selected and restricted between November and March (Figure
178 1b) in order to minimize the aliasing of the seasonal variability due to the lack of in situ data
179 in other seasons than summer. The data consist of seawater temperature, practical salinity, and
180 dissolved oxygen (DO). Conservative temperature (Θ; ^{o}C) and absolute salinity (S_A; g kg^{-1})
181 were calculated from TEOS–10 (McDougall et al., 2011), as well as neutral density (γ^n; kg m^{-}

^{3}; Jackett & McDougall, 1997). Only data from the eastern and central Bransfield Strait basins were considered. To avoid the influence from other coastal processes, only regions where the bathymetry was greater than 500 m were considered (using the IBCSO v1.0; https://www.scar.org/science/ibcso/). Duplicate hydrographic stations appearing in more than one data set were identified and removed from the analyzes, as well as spurious data (i.e., property values greater than two standard deviations for each profile).

The data sets were split by their respective basins (central and eastern; Figure 1b) to produce the time series as follows. Profiles of anomaly of the thermohaline properties for both basins were calculated relative to the averaged profile from the years 2000 to 2019. The choice of this time interval is related to the greater temporal and spatial data coverage within the time series. After calculating the anomaly profiles, each profile was grouped according to its summer season, and the average annual value and standard deviation were calculated for each property. The central basin time series spans 1963 to 2019, while the eastern basin covers the period of 1975 to 2019. Next, we used a second threshold to analyze just the water layer with $\gamma^n \geq 28.27$ kg m^{-3} and depths greater than 800 m. The restrictions used helped to select only the deep water masses of the Bransfield Strait that preserve their original thermohaline characteristics acquired on the Weddell Sea continental shelf, thus analyzing the water masses in their "pure" forms by isolating them from the effects of mixtures and favoring the observation of clearer signals (Dotto et al., 2016).

2.2. Ancillary data set

The SAM (https://climatedataguide.ucar.edu/climate–data/marshall–southern–annular–mode–sam–index; Marshall, 2003) and the monthly Bivariate ENSO time–series (https://www.psl.noaa.gov//people/cathy.smith/best; Smith & Sardeshmuk, 2000) indices were used to study the relationships between the thermohaline properties of the Bransfield Strait

deep waters and the large-scale climate modes. In addition, monthly sea ice concentration (SIC) data were taken from the U.S. National Snow and Ice Data Center, processed with the NASA Team algorithm 1.1 (Cavalieri et al., 1984). Additionally, SIC anomalies relative to 1979 to 2018 were computed for the Weddell Sea as a proxy for sea ice formation.

Wind velocity components, 10-m absolute wind speed (U) and 2 m air temperature (T) were obtained from the European Centre for Medium–Range Weather Forecast Reanalysis (ERA5; https://cds.climate.copernicus.eu/cdsapp#!/home; Hersbach et al., 2020). The open ocean heat loss anomalies relative to 1979 to 2018 were computed for the Weddell Sea as a proxy for sea ice formation rate (SFR) using the bulk formula (Eq. 1), following Hatterman et al. (2021):

$$SFR = \rho^a C_p^a C_s \times (1 - SIC) \times U \times \Delta T, \quad (1)$$

where ρ^a is air density (ρ^a = 1.3 kg m^{-3}), C_p^a is the specific heat capacity of air (C_p^a = 10^3 J kg^{-1} K^{-1}), C_s is the sensible heat transfer coefficient (C_s = 1.5 x 10^{-3}), and the difference between the 2 m air temperature and the ocean surface freezing temperature, computed as $\Delta T = -1.9^{\circ}C - T$. Moreover, wind velocity components anomalies relative to 1979 to 2018 summer period were computed for the Weddell Sea.

2.3. Water masses fractions of mixture

The Optimum Multiparameter Analysis (OMP) inverse method (Tomczak & Large, 1989) was used to quantify the percentage of mixing between different water masses in the Bransfield Strait. The OMP method was used here to analyze the source waters contribution to the water mixture in the deep layers (i.e., depths > 800 m) for a hydrographic section crossing the central and eastern basins (Figure 1b) and was applied to the high–resolution data obtained

by the GOAL in the years 2004, 2008–2010, 2013–2016, and 2019, because of the availability of DO data to run the mixing model.

The source water types (i.e., the conservative and/or semiconservative parameter values that represent a water mass in its source region) chosen were CDW, LSSW, and HSSW. The former representing all the modified varieties derived from CDW, while the later representing the Dense Shelf Water varieties derived from the Weddell Sea continental shelf. The source water types indices originally determined through the EOS–80 routines (Dotto et al., 2016), were transformed here through the application of TEOS–10 (Table 1). The parameter weights were determined according to Tomczak and Large (1989) and remained similar for the two sets of indices derived from the older and recent seawater state equations (Table 1 and Dotto et al., 2016). Finally, sensitivity tests were performed using the Monte Carlo method to randomly varying the source water types index values to support the robustness of the results (e.g., Almeida et al., 2018, Kerr et al., 2018b). The results were considered reliable due to the low residual of mass conservation found for all OMP runs (< 5%).

Table 1. Source water type indices and the respective weights obtained from TEOS–10 for each hydrographic property used in the OMP analysis. The water masses represented are High Salinity Shelf Water – HSSW, Low Salinity Shelf Water – LSSW, and Circumpolar Deep Water – CDW. The parameters are conservative temperature (Θ), absolute salinity (S_A), and dissolved oxygen (DO). [a] Weight applied for mass conservation.

Parameters	Source Water Type			
	HSSW	**LSSW**	**CDW**	**Weights**
Θ (˚C)	$-1.88 \leq \Theta \leq -1.70$	$-1.88 \leq \Theta \leq -1.70$	$0 \leq \Theta \leq 1$	1.0730
S_A (g kg^{-1})	$34.73 \leq S_A \leq 35.01$	$34.56 \leq S_A \leq 34.46$	$34.77 \leq S_A \leq 34.92$	1.0730
DO (µM)	$326 \leq DO \leq 308$	$330 \leq DO \leq 321$	$219 \leq DO \leq 192$	2.2502[a]

3. Results

3.1. Trends and variability of the deep waters of the Bransfield Strait (1960s –2010s)

252 The Bransfield Strait central basin showed a significant ($p<0.05$) long–term cooling of
253 $–0.0021 \pm 0.0020$ºC $yr^{–1}$, freshening of $–0.0005 \pm 0.0005$ g $kg^{–1}$ $yr^{–1}$, lightening of $–0.0011 \pm$
254 0.0010 kg $m^{–3}$ $yr^{–1}$, and deepening of the 28.27 kg $m^{–3}$ isopycnal of $–4.92 \pm 3.99$ m yr^{-1} from
255 1963–2019 (Figure 2). Moreover, the decrease in DO of $–0.0022 \pm 0.0086$ mL $L^{–1}$ $yr^{–1}$ was not
256 statistically significant. Considering the Bransfield Strait eastern basin (Figure 3), significant
257 long-term trends were observed for S_A ($–0.0007 \pm 0.0005$ g $kg^{–1}$ $yr^{–1}$) and γ^n ($–0.0017 \pm 0.0012$
258 kg $m^{–3}$ $yr^{–1}$). The deepening of the 28.27 kg $m^{–3}$ isopycnal was threefold higher ($–15.32 \pm 9.59$
259 m $yr^{–1}$) than in the central basin, and a significant DO decrease trend of $–0.0136 \pm 0.0077$ mL
260 $L^{–1}$ $yr^{–1}$ was observed (Figure 3e).
261

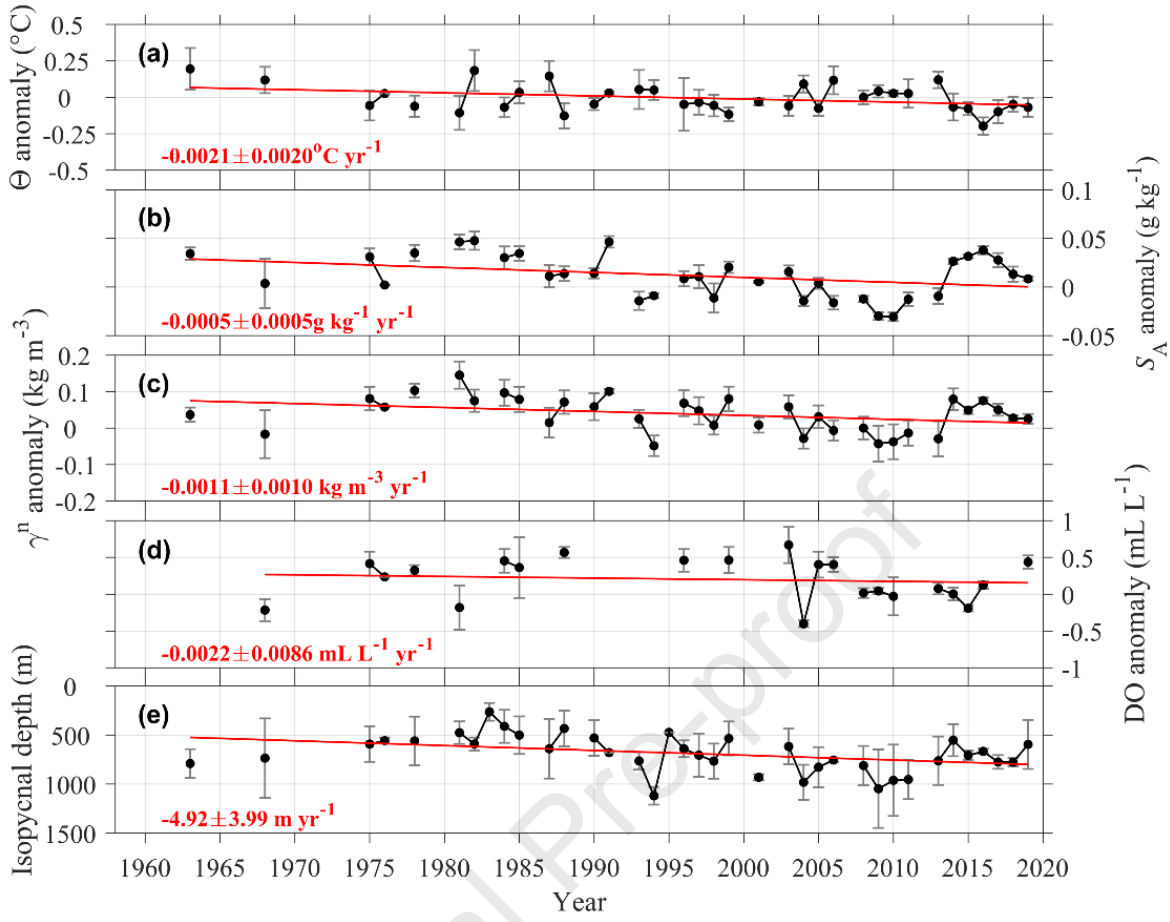

262

263 **Figure 2.** Anomaly time series of the hydrographic parameters for the deep waters ($\gamma^n \geq 28.27$
264 kg m^{-3} and depth > 800 m) in the central basin of the Bransfield Strait. (a) Conservative
265 temperature (Θ), (b) Absolute salinity (S_A), (c) neutral density (γ^n), (d) dissolved oxygen (DO),
266 and (e) the depth of the 28.27 kg m^{-3} isopycnal. The grey error bars show the annual standard
267 deviation. The linear trends are depicted by the red lines within each plot. The linear trends and
268 confidence bounds are shown in the left bottom corner of each panel. For time series of the
269 absolute hydrographic parameters for the deep waters of the Bransfield Strait central basin,
270 please refer to supporting information Figure S2.

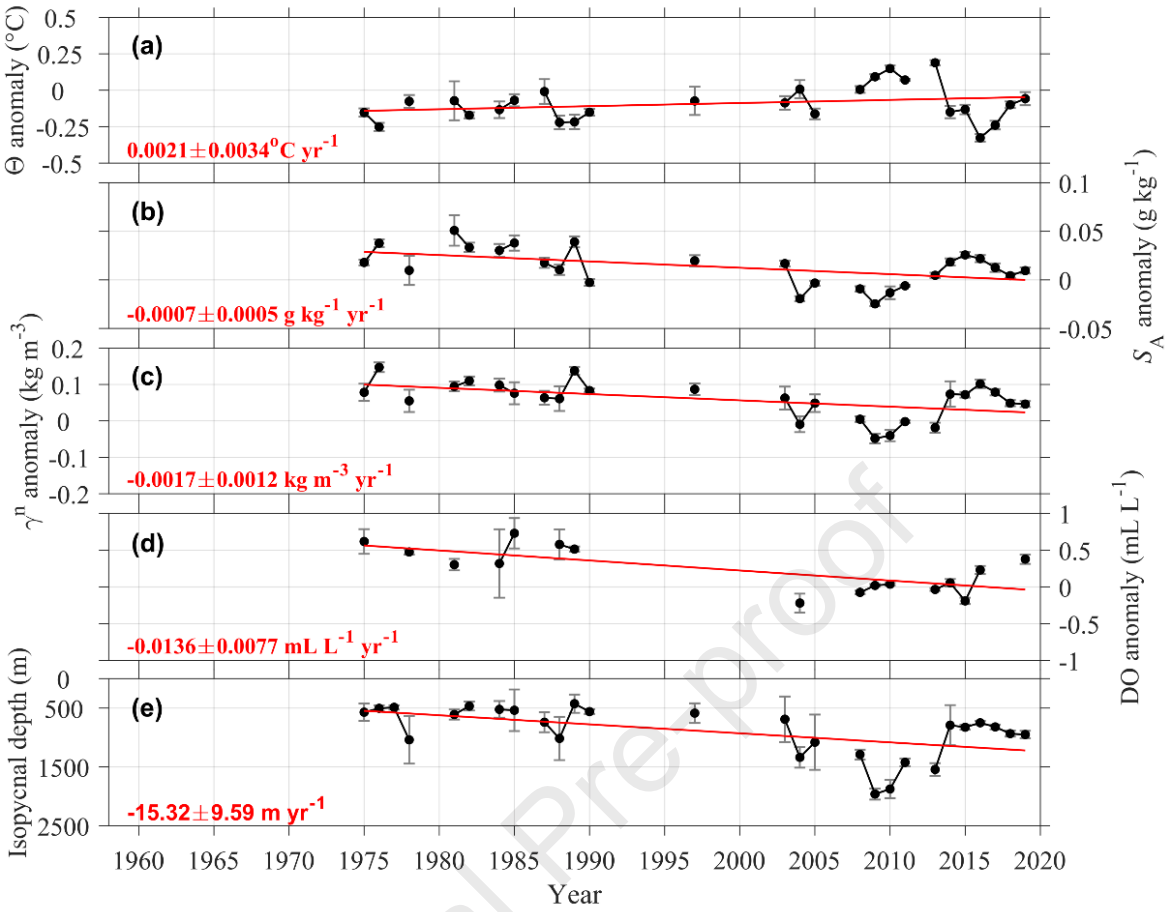

Figure 3. Anomaly time series of the hydrographic parameters for the deep waters ($\gamma^n \geq 28.27$ kg m^{-3} and depth > 800 m) in the eastern basin of the Bransfield Strait. (a) Conservative temperature (Θ), (b) Absolute salinity (S_A), (c) neutral density (γ^n), (d) dissolved oxygen (DO), and **(e)** the depth of the 28.27 kg m^{-3} isopycnal. The grey error bars show the annual standard deviation. The linear trends are depicted by the red lines within each plot. The linear trends and confidence bounds are shown in the left bottom corner of each panel. For time series of the absolute hydrographic parameters for the deep waters of the Bransfield Strait eastern basin, please refer to supporting information Figure S3.

The deep waters of the central and eastern basins showed considerable freshening and lightening between 1980 to 2010 (Figures 2b–2c and 3b–3c), when the lowest values in the time series were reached. The average S_A in 2010 was 34.69 and 34.70 g kg^{-1} for the central and eastern basins, respectively (Figures S2b and S3b). Between 2010 and 2016, the deep layers of the Bransfield Strait showed an increase in S_A in both the central and the eastern basins at rates of 0.0117 ± 0.0050 g kg^{-1} yr^{-1} and 0.0660 ± 0.0024 g kg^{-1} yr^{-1}, respectively (Table 2). Moreover, in 2016 the average S_A was 34.76 and 34.74 g kg^{-1} for the central and

eastern basins, respectively, comparable to the magnitudes of those of the 1980s (Figures 2b, 3b, S2 and S3). From 2016 to 2019, the S_A of the deep layers of the central and eastern basins declined again at rates of –0.0103 ± 0.0056 g kg^{-1} yr^{-1} and –0.0045 ± 0.0105 g kg^{-1} yr^{-1}, respectively (Table 2), when an averaged S_A of 34.69 g kg^{-1} was registered for both basins in 2019 (Figures S2 and S3). This observed pattern in the salinity field between 2010 and 2019 was followed by γ^n (Figures 2b and 3b) and mirrored by Θ (Figures 2a and 3a).

Table 2. Trends and confidence levels of the conservative temperature (Θ), absolute salinity (S_A), neutral density (γ^n), dissolved oxygen (DO), and the γ^n of 28.27 kg m^{-3} isopycnal depth observed in the Bransfield Strait central and eastern basins for different periods. The p–values are presented in parentheses. Significant trends at 95% confidence level are indicated by bold values.

Hydrographic properties	Central Basin	Eastern Basin
	Trends(1960s–2019)	
Θ (˚C)	**–0.0021 ± 0.0020 (0.04)**	–0.0021 ± 0.0034 (0.20)
S_A (g kg^{-1})	**–0.0005 ± 0.0005 (0.04)**	**–0.0007 ± 0.0005 (0.01)**
γ^n (kg m^{-3})	**–0.0011 ± 0.0010 (0.04)**	**–0.0017 ± 0.0012 (0.01)**
DO (mL L^{-1} yr^{-1})	–0.0022 ± 0.0086 (0.6)	**–0.0136 ± 0.0077 (0.00)**
Isopycnal depth (m yr^{-1})	**–4.92 ± 3.99 (0.02)**	**–15.32 ± 9.59 (0.00)**
	Trends (2010–2016)	
S_A (g kg^{-1})	**0.0117 ± 0.0050 (0.00)**	**0.0066 ± 0.0024 (0.00)**
γ^n (kg m^{-3})	**0.0195 ± 0.0173 (0.03)**	**0.0229 ± 0.0146 (0.01)**
	Trends (2016–2019)	
S_A (g kg^{-1})	**–0.0103 ± 0.0056 (0.02)**	–0.0045 ± 0.0105 (0.21)
γ^n (kg m^{-3})	**–0.0173 ± 0.0167 (0.05)**	**–0.0197 ± 0.0175 (0.04)**

3.2 Variability in the contribution of the Bransfield Strait deep waters mixture

The averaged contribution of the deep water masses in the Bransfield Strait deep layers between 2004 and 2019 had the following mixing fractions: (i) CDW contributed ~31 ± 10% in the central basin and ~44 ± 8% in the eastern basin; (ii) HSSW contributed ~31 ± 12% in the central basin and ~18 ± 9% in the eastern basin, and (iii) the LSSW contributed ~38 ± 7% in both basins (Figure 4). Furthermore, the strongest intrusion of HSSW into the two basins of the Bransfield Strait during the analyzed period occurred in 2016 and 2019 (Figures 5 and S4),

whereas the highest contribution of LSSW was observed in 2009 (Figures 5 and S4). On the other hand, the largest contribution of CDW into the two basins of the Bransfield Strait was observed in 2004 and 2015 (Figures 5 and S4). Besides, an averaged difference of up to ~1.5% was found for the period 2004–2019 comparing the contribution of water masses between the thermodynamic equations EOS–80 and TEOS–10 (Figure S5).

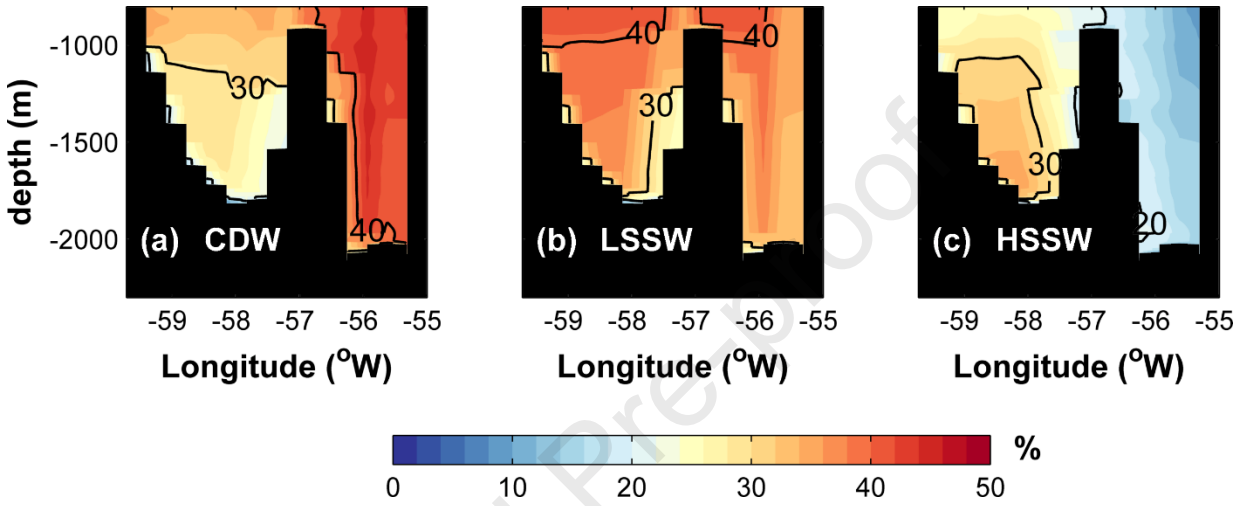

Figure 4. Time-averaged source water masses contribution (%) to the deep waters of the Bransfield Strait, over the 9 years analyzed (2004–2019). (a) Circumpolar Deep Water (CDW), (b) Low Salinity Shelf Water (LSSW), (c) High Salinity Shelf Water (HSSW). For the interannual contribution, please refer to supporting information Figure S5.

The contributions of the CDW and LSSW decreased by ~33% and ~5% in the central basin between 2004 and 2019, respectively (Figure 5a). Conversely, the HSSW increased ~38% for the same period at the same location. For the eastern basin, CDW and LSSW decreased by ~25% and ~5%, respectively, whereas HSSW increased ~28% between 2004 and 2019 (Figure 5b).

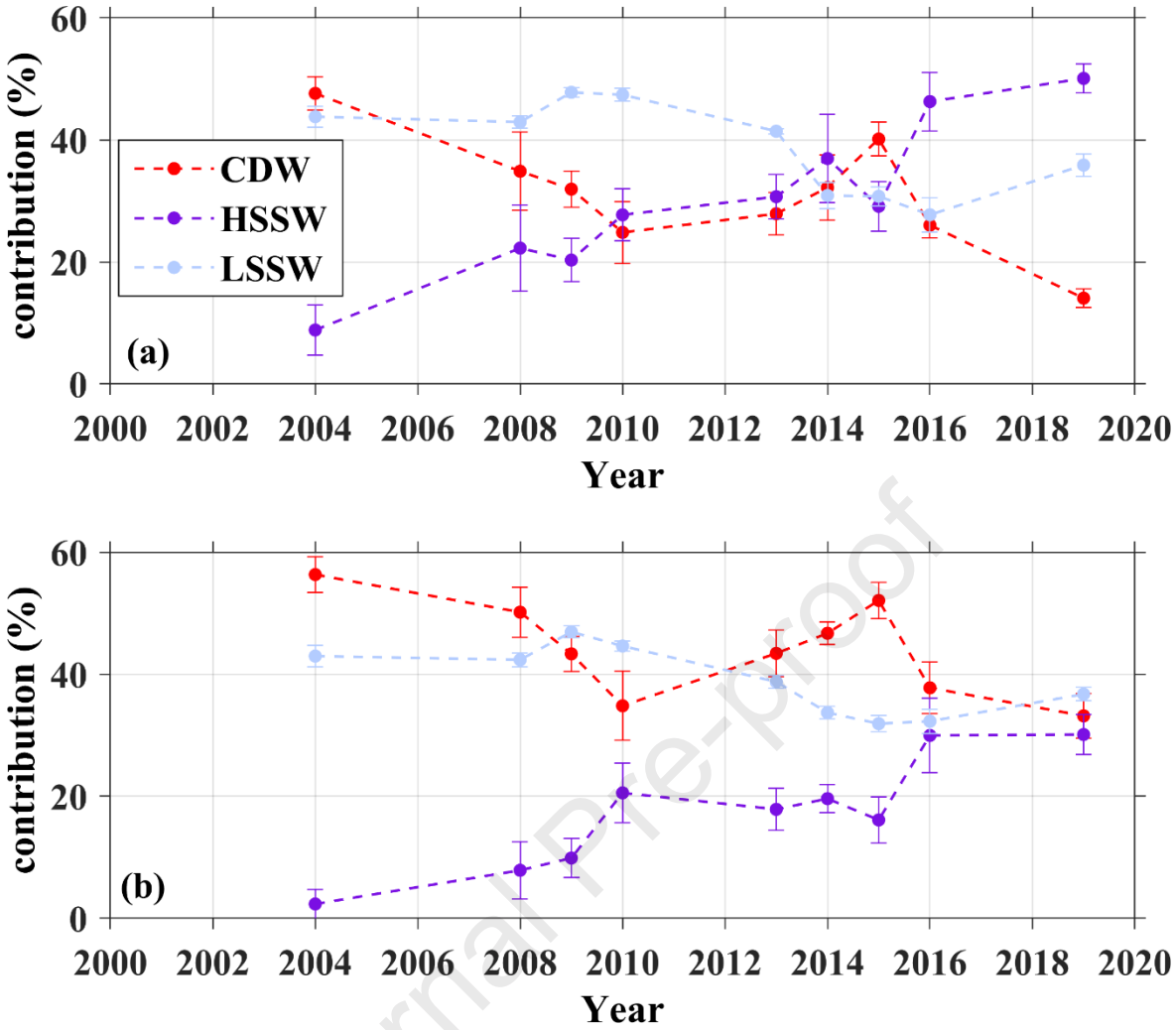

Figure 5. Time series of the average contribution (%) of the source water masses observed in the (a) central basin and the (b) eastern basin of the Bransfield Strait. CDW (red), HSSW (blue), and LSSW (cyan). The error bars indicate the respective standard deviations. These results were generated from TEOS–10.

3.3 Relationship between the climate modes and deep water masses variability in Bransfield Strait

The correlations between the normalized and detrended thermohaline properties of the Bransfield Strait central and eastern basins and SAM/ENSO indices were tested from 2004 to 2019. This period was chosen because of the greater temporal and spatial resolution concerning the whole data set. Different time-lags were applied, and the best correlations were identified in a 5-months lag between the time series, a period similar to that found by Jullion et al. (2010) and Dotto et al. (2016). This interval indicates that the hydrographic properties obtained during

339 the austral summer within the Bransfield Strait are correlated with the SAM and ENSO indices
340 from August to October of the previous year.

341 The γ^n of the central basin was significantly anti-correlated to the SAM index (r = –
342 0.56 at the >95% statistical significance level; Table S1). This suggests that positive phases of
343 SAM leads to a decrease in water density in the central basin of the Bransfield Strait in the
344 following summer, whereas a negative SAM leads to an increase in deep water density in the
345 Bransfield Strait central basin. On the other hand, S_A and Θ for both basins and γ^n of the eastern
346 basin were not significantly correlated to SAM (Table S1).

347 Regarding ENSO, the correlations showed an opposite pattern compared to SAM,
348 although not significant for any property (Table S1). The lack of statistical significance may
349 be attributed to the reduced number of years considered for this analysis (N=15) due to the
350 temporal gaps in the full hydrographic time series. Hence, considering only the general
351 correlation pattern, El Niño (La Niña) leads to a decrease (increase) in temperature, and an
352 increase (decrease) in salinity and density in both basins.

353

354 **4. Discussion**

355 **4.1. Long–term freshening and salinity changes on deep Bransfield Strait basins**

356 The Bransfield Strait is a region under the influence of different water masses,
357 oceanographic and biogeochemical regimes (e.g., Collares et al., 2018; Ito et al., 2018, Kerr et
358 al., 2018a; Dotto et al. 2021). Its deep basins have particular conditions because the varieties
359 of the Dense Shelf Water that are advected into the strait sink in depths with little mixing with
360 the surrounding water masses. This allows the local Bransfield Strait deep water masses to
361 keep their original thermohaline properties for longer periods, which is useful to study the
362 temporal variability of the source water masses (Dotto et al., 2016). Several studies have shown
363 that the water masses of the region are freshening and lightening since at least the 1960s (e.g.,

Garcia and Mata, 2005; Azaneu et al., 2013; Dotto et al., 2016; Ruiz Barlett et al., 2018). For instance, Dotto et al. (2016) reported a freshening trend of –0.0010 ± 0.0005 yr^{-1} for the Bransfield Strait central basin (between 1963 and 2014) and –0.0010 ± 0.0006 yr^{-1} for the Bransfield Strait eastern basin (between 1975 and 2014). Moreover, they showed a lightening –0.0016 ± 0.0014 kg m^{-3} yr^{-1} and –0.0029 ± 0.0013 kg m^{-3} yr^{-1} for the Bransfield Strait central and eastern basins, respectively, for the same periods. Here, the observed freshening and lightening rates continued until 2019. However, the magnitude of these rates is smaller than the ones found previously. The, new rates are: (i) freshening of –0.0005 ± 0.0005 g kg^{-1} yr^{-1} and lightening –0.0011 ± 0.0010 kg m^{-3} yr^{-1} for the central basin, and (ii) freshening of –0.0007 ± 0.0005 g kg^{-1} yr^{-1} and lightening of –0.0017 ± 0.0012 kg m^{-3} yr^{-1} for the eastern basin (Figures 2b-c and 3b-c). Additionally, we also showed that the increase in salinity and density reported by Dotto et al. (2016), which started in 2010, continued until 2016 when a new drop in these properties occurred.

The freshening trends observed in the Bransfield Strait may be linked with the melting of ice shelves and glaciers around the western Weddell Sea in the last 50 years (Cook et al., 2016; Shepherd et al., 2018; Jullion et a., 2013; Paolo et al., 2015; Rignot et al., 2019). For example, a freshwater discharge of ~24 Gt yr^{-1} was estimated for the western Weddell Sea, which was caused by the disruption of the Larsen ice shelves between 1979 and 2017 (Rignot et al., 2019). Such discharge is likely the main cause of the averaged regional freshening rate of ~ –0.0006 g kg^{-1} yr^{-1} for the Bransfield Strait central and eastern deep layers found here. Several areas in Antarctic have shown an increase in melting rates of ice shelves, resulting in a general mass loss (Paolo et al., 2015). Consequently, large volumes of the continental freshwater are injected into the ocean (Rignot et al., 2019). Thus, this excess of the continental freshwater released impacts the Antarctic coastal system, as evidenced by the Southern Ocean circumpolar freshening reported in many areas (Jacobs & Giulivi, 2010; Hellmer et, al., 2011;

Azaneu et al., 2013; Kusahara et al., 2014; Schmidtko et al., 2014; Aoki et al., 2020a). For the Weddell Sea continental shelf, long–term freshening trends of −0.0013 yr^{-1} and −0.0010 g $kg^{-1}yr^{-1}$ have been reported by Azaneu et al. (2013) and Schmidtko et al. (2014), respectively, between the 1980s and 2010.

Given the changes in the salinity and density fields, a shrinking of the deep waters layer is occurring in the Bransfield Strait. The depth of the isopycnal of 28.27 kg m^{-3} (a level which is normally used as the upper limit for the AABW layer) in the central and eastern basins deepened, respectively, at rates of –4.92 ± 3.99 m yr^{-1} and –15.32 ± 9.59 m yr^{-1} (Figures 2e and 3e) between the 1960s and 2019. Our results are consistent with Dotto et al. (2016), which found –5.60 ± 5.27 m yr^{-1} and –24.98 ± 11.09 m yr^{-1} until 2014 for the central and eastern basins, respectively. The shrinking of the deep water mass layers in the Bransfield Strait seems to fit in the global contraction scenario of the AABW (Jacobs et al., 2010; Purkey & Johnson, 2013; Jullion et al., 2013; van Wijk et al., 2014; Abrahamsen et al., 2019). This indicates that the source composition of AABW (Kerr et al. 2018b) are crucial to evaluate changes in the volume produced and, consequently, exported of such water mass to the lower limb of the global overturning circulation. If lightening trends continue steadily, it is expected that in ~118 years, the γ^n of the central basin will reach values lower than 28.27 kg m^{-3}. Nevertheless, it is still unclear if the trends observed are being caused by changes in the central basin deep waters ventilation, as no trend was observed for DO (Figure 2d). In the eastern basin, DO has decreased likely associated with the warming observed in that basin (Figure 3a and 3d). Overall, the volume shrinking reported here appears to be linked to the freshening and lightening trends, once freshening can drive water mass contraction even if the overall formation rate remains unchanged (van Wijk & Rintoul, 2014; Dotto et al., 2016).

From 2010 to 2016, there was a remarkable salinity increase in the deep waters of the Bransfield Strait, suggesting a small recovery in the volume of these dense waters in both

basins (Figures 2b-2e and 3b-3e). The OMP analysis suggested that the recovery was related with a greater contribution of HSSW between 2010 and 2016. Moreover, this salinization has been also reported later for the Ross Sea coastal region after 2015 (Castagno et al., 2019; Silvano et al., 2020). Associated with the Ross Sea salinity increase, Aoki et al. (2020b) also reported a reversal of the AABW dilution trend in the Antarctic–Australian basin between 2011 and 2018. Thus, this variability in the salinity field may be linked to a circumpolar change in the properties of the shelf waters. However, here we show that the reversal freshening stopped in 2016, and since then, the salinity decreased again. Nevertheless, understanding whether the pan-Antarctic coastal freshening will continue after the reversal freshening period that have been recently described (e.g., Catagno et al., 2019; Aoki et al., 2020b; Silvano et al., 2020) is a task for future studies.

4.2. Variability of the deep water masses of the Bransfield Strait linked to sea ice formation

The increasing of HSSW contribution in the central and eastern basins by ~28 and 38% was observed between 2004 and 2019, respectively, while LSSW reduced ~5% for both basins for the same period. Conversely, CDW reduced by 33 and 25% for the same period for the central and eastern basins, respectively (Figure 5). Moreover, our results show that the increase in S_A from 2010 to 2016 is linked to the higher contribution of ~17% in the HSSW (Figure 5). This increase had already been noted by Dotto et al. (2016), but the temporal extension of the sign of the reversal freshening was still not evident in that study. Between 2016 and 2019, the decrease in S_A is linked to an ~11% increase in the contribution of LSSW and a ~12% reduction in CDW inside the Bransfield Strait (even though there was a ~1% increase in HSSW for the period). Thus, the role of sea ice in both the northwestern Weddell Sea and S_A of the central and eastern basins are further analyzed to verify if the increase in contribution of HSSW (and

439 therefore salinity) between 2010 and 2016 was potentially caused by the sea ice formation
440 (Fahrbach et al., 1994; Tamura et al., 2011; Abernathey et al., 2016).

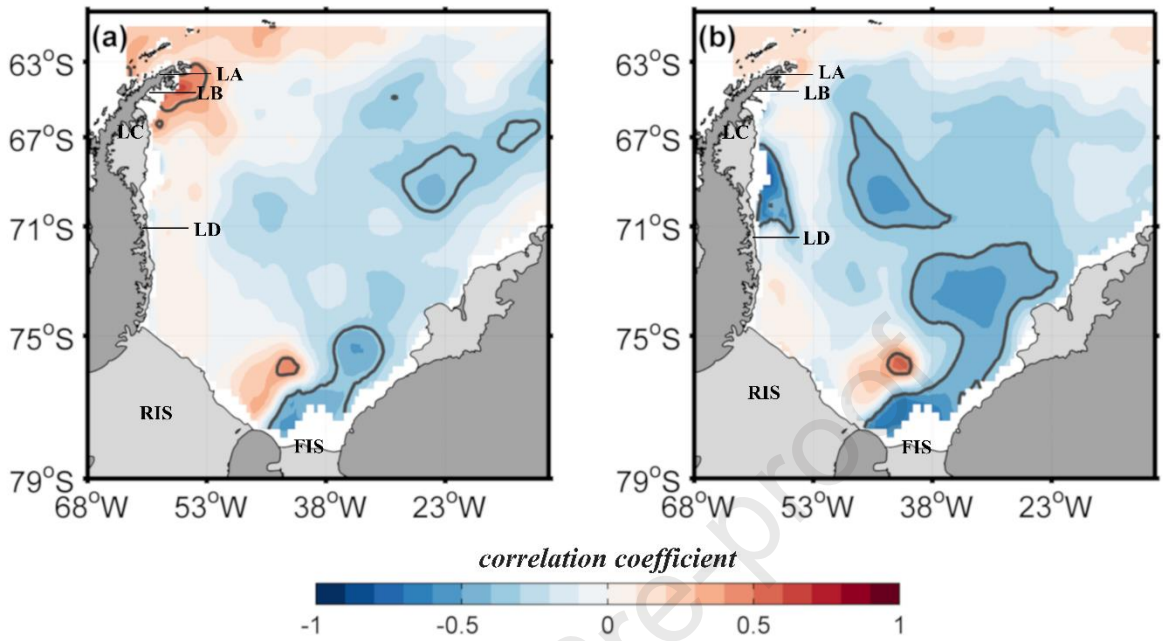

441
442 **Figure 6.** Correlation maps between sea ice formation rates (SFR) in the southern winter period
443 (August to October) and absolute salinity (S_A) for the (a) central and (b) eastern basins of the
444 Bransfield Strait. The black line shows p-values of 0.05. The period analyzed for the correlation
445 was made between 1979 and 2018. In addition, the SFR leads S_A by on year. The Labelled ice
446 shelves are Larsen A, B, C and D (LA, LB, LC and LD), Ronne Ice Shelf (RIS) and Filchner
447 Ice Shelf (FIS).
448
449 It is a remarkable agreement between the time series of area-averaged SFR and SIC in
450 the Weddell Sea region (Figures 7 and S6). Thus, we used SFR as a proxy for salinification of
451 shelf waters and sea ice formation in the region. In this context, a significant positive
452 correlation between the SFR near the Larsen Ice Shelf and S_A for the Bransfield Strait central
453 basin (r ~ 0.65; Figure 6a) was found between 1979 and 2018, suggesting that higher salinity
454 in the deep Bransfield Strait central basin is mainly associated with higher SFR at the
455 northwestern Weddell Sea from the previous winter. These results are consistent with van
456 Caspel et al. (2018), which indicated through model analysis that the deep waters of the
457 Bransfield Strait central basin are under the influence of the water masses produced at the
458 western Weddell Sea continental shelf. Furthermore, it is noticeable the agreement between the
459 central basin S_A time series and the area-averaged SFR time series in the Weddell Sea region

(Figures 7a). This suggests that the increase of SFR can favour the injection of salt in the shelf waters by brine rejection mechanism during its formation, contributing to a potential increase in the concentration of salt in shelf waters and, consequently, in deep waters of the Bransfield Strait. Moreover, a marked SFR increase is evident in the region during the period spanning from 2010 to 2019 (Figure 7a; note that the SFR is advanced one year in the figures), which corroborates with the reversal of the freshening signal that had been occurring in the deep waters of the Bransfield Strait between 2010 and 2016. In 2017, there was a further reduction in SFR in the region (Figure 7), which was followed by a reduction in S_A in the central basin since 2017.

Similarly, a significant positive correlation between SFR near the region of Ronne-Filchner ice shelves and S_A in the eastern basin of the Bransfield Strait (r ~0.57; Figure 6b) was verified for the period spanning from 1979 to 2018. Thus, the observed results reported here highlight the robustness of the modeling outputs and hypothesis raised by van Caspel et al. (2018), who indicated that the eastern basin of the Bransfield Strait is under the influence of water masses produced further south on the southern Weddell Sea shelves (i.e., closer to Ronne-Filchner ice shelves). Thus, indicating that the eastern basin of the Bransfield Strait can be highly fed by Dense Shelf Water varieties transported by the changing dynamics of the Antarctic Slope Front (Thompson et al., 2009; Heywood et al., 2014), which can result from mixture with Ice Shelf Water (Nicholls et al., 2009) and explain the recurrent and still unresolved report of different hydrographic properties between the basins (Wilson et al., 1999; Gordon et al., 2000; Dotto et al., 2016). Like the Bransfield Strait central basin, the eastern basin salinity also revealed an agreement with the area-averaged SFR at the Weddell Sea (Figure 7b). Also, it is noteworthy that salty variety of Dense Shelf Water forms because of sea ice production on the southwestern Weddell Sea off Ronne Ice Shelf (Haid & Timmermann, 2013). Thus, the areas that showed a negative correlation between salinity in the deep waters

485 of the Bransfield Strait and sea ice formation in front of the Filchner Ice Shelf can be
486 disregarded.

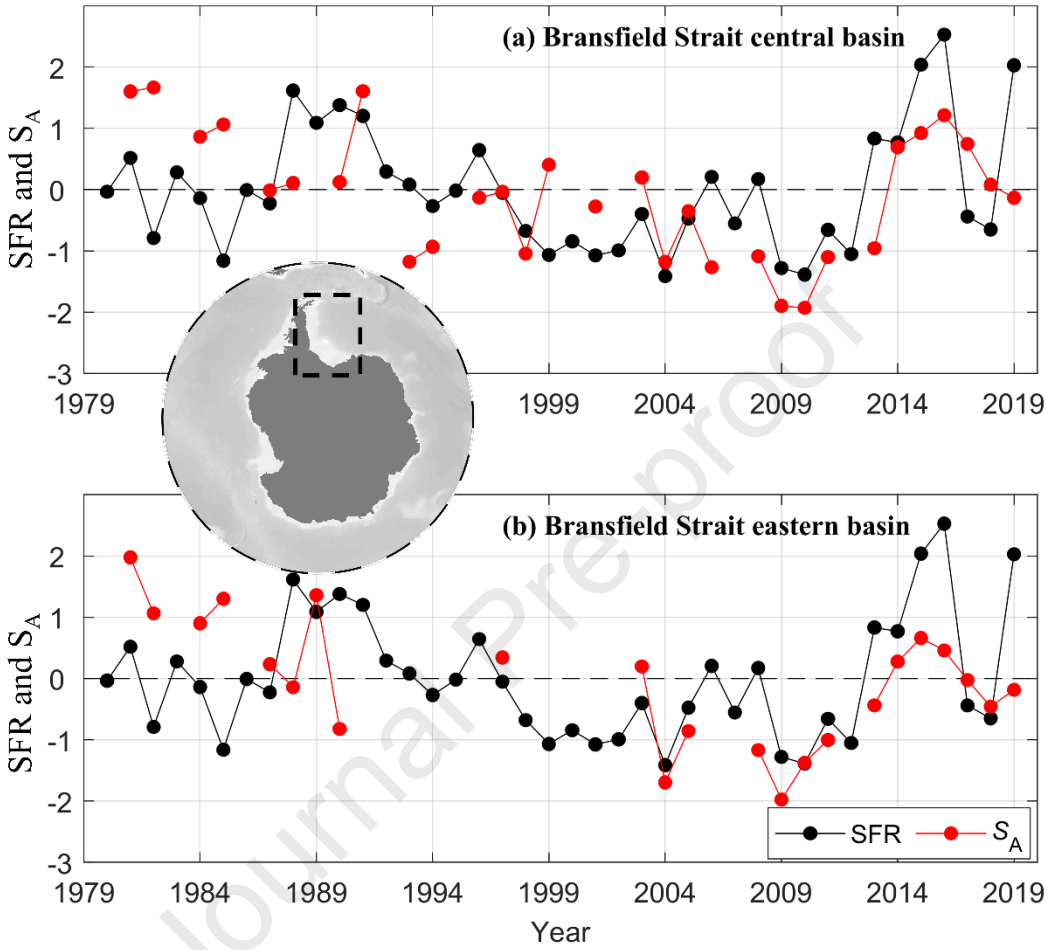

487

488 **Figure 7.** Normalized and detrended time series of the mean sea ice formation rates (SFR)
489 anomalies in the southern winter period (August to October) in the Weddell Sea region (black
490 dots) and the absolute salinity (S_A) anomaly (red dots) for the (a) central and (b) eastern basins
491 of the Bransfield Strait. The mean SFR anomalies are calculated within the black area
492 represented in the inset. Note that the SFR leads S_A by on year in the figure. The anomalies are
493 referenced to the 1979-2018 southern winter period.

494

495 **4.3. The role of the wind pattern driven by climate modes**

496 The wind patterns over the Weddell Sea, which are associated with SAM and ENSO
497 climate modes, have a key importance in the formation and export variability of the shelf water
498 masses (Gordon et al., 2010; McKee et al., 2011). It is suggested that La Niña events and
499 negative SAM conditions are associated with the weakening of both (i) the south-westerly

winds at the southern Weddell Sea (Turner et al., 2020) and (ii) the Antarctic Coastal Current system (Youngs et al., 2015), consequently leading to less sea ice export to the northwestern Weddell Sea (Figure 8a and 8c). The period between 2006 and 2009 was marked by a transition from El Niño to La Niña and a negative SAM phase (Figure S7). As a result, sea ice is accumulated along the western continental shelf of the Weddell Sea (Figure 8a), restricting ocean-atmosphere interaction, and hence reducing the formation rate of HSSW due to less sea ice formation (Figure 7). This proposed mechanism agrees with the low concentration of HSSW (~20%) on the Bransfield Strait deep waters from 2006 to 2009 (Figures 5 and S4).

The opposite scenario occurs during El Niño events and positive SAM phases. The interaction of these modes is associated with a stronger southerly wind in the Weddell Sea (Yuan et al., 2018; Meijers et al., 2019), as observed during the years of 2010 and 2018, a period marked by a positive SAM phase and the transition from La Niña to El Niño (Figures 8b and S7). It suggests a potential increase in the export of sea ice from the Weddell Sea across the Antarctic Coastal Current system (Mckee et al., 2011; Turner et al., 2020; Kumar et al., 2021), as noted in Fig. 8b-c. Hence, stronger southerly winds that might be connected to a positive SAM and El Niño events (e.g., extreme El Niño during 2015; Figure S7) increase open ocean areas, which rises turbulence and heat loss, resulting in favorable conditions for sea ice formation (Liu et al., 2004). That facilitates increment in the production of HSSW through sea ice brine rejection on subsurface waters over the western Weddell Sea continental shelf (e.g., Tamura et al., 2011), which could be later exported towards Bransfield Strait (van Caspel et al., 2018).

Overall, our results are consistent with Hattermann et al. (2021), who showed that enhanced sea ice formation is associated with stronger south-westerly winds over the Ronne Ice Shelf. It is also expected that the export of HSSW formed in the Weddell Sea (approximately 76.22ºS/054.80ºW) occurs through gravity plumes and will flow northward

525 with a velocity of approximately 12 cm s^{-1} (e.g., Gordon et al., 2010; McKee et al., 2011).
526 Thus, these waters can reach the deep basins of the Bransfield Strait (approximately
527 62.90ºS/057.64ºW) in ~5 months. This period is in line with Collares et al. (2018), who
528 estimated that medium-sized icebergs would take ~6 months to move from the northwestern
529 Weddell Sea (65.90°S/055.3°W) to the boundary between the southern Bransfield and
530 Gerlache Straits (64.20°S/061.8°W). Moreover, our results are in consonance with those
531 proposed by Barbat et al. (2021), who estimated that larger-sized icebergs would take ~12
532 months to move from the Ronne-Filchner ice shelves to the northwestern Weddell Sea.

533

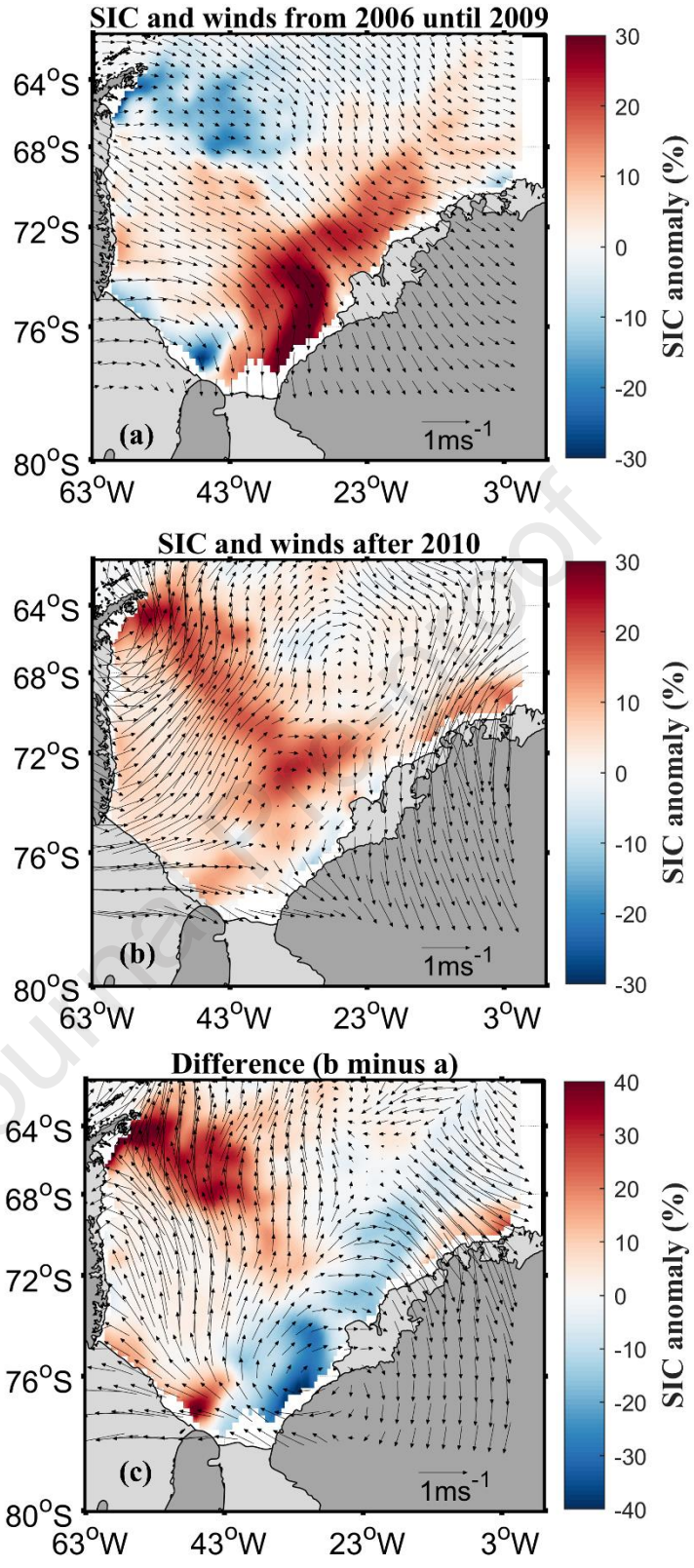

534

535 **Figure 8.** Map of the average anomalies of the sea ice concentration (SIC) in the summer
536 period (January and February) with the black arrows representing the average of the anomalies
537 of the wind speed in the 10 m in the southern summer period (January and February).
538 Anomalies of the winds and SIC for the period from (a) 2003 to 2009, (b) 2010 to 2018, (c)
539 difference from panels b and a. The anomalies are referenced to the 1979-2018 summer period.

In the northwestern Weddell Sea (near the region off Larsen Ice Shelves A and B) the SIC increases post-2010 (Figure 8b and c). Afterward, such high concentration of sea ice has the potential to melt and accumulate freshwater along the coast. This excess of freshwater might mix with coastal Winter Water and form LSSW (Zhou et al., 2014). Therefore, the freshening sign that occurred in the Bransfield Strait deep waters after 2016 corroborates with this scenario (Figures 2b and 3b). These processes agree with the water masses fractions of mixture (Figures 4, 5, and S4), as observed by a significant increase of LSSW during the same period. However, even with the robust results of the water masses fractions of mixture, which varied the source water types indexes within the range that define each of Dense Shelf Water varieties, the hypothesis that the increase in the LSSW contribution would be related to an increase in the contribution of a modified HSSW (i.e., fresher due to mixing with ambient waters) cannot be completely discarded, being a challenge and open question for future studies.

Finally, the recent reversal salinity trend reported here was also observed in the Ross Sea between 2015 and 2018, being explained by the interannual variability in sea ice production and further export (Castagno et al., 2019; Silvano et al., 2020). Those sea ice processes were associated to be caused by the combined effects of ENSO and SAM modes. However, the hypothesis of a variation in the local ocean circulation, which could be accelerated due to the intensification of winds, is not ruled out. In this case, the inflow of Dense Shelf Water varieties into the Bransfield Strait would happen more quickly, resulting in less time for mixing the coastal waters with the adjacent waters. Therefore, continuous in situ observations to investigate the local deep circulation are necessary to assess those effects in the region.

5. Concluding remarks

In this study, we showed that the deep water masses of the central (1963–2019) and eastern (1975–2019) basins of the Bransfield Strait experienced significant rates of freshening of –0.0005 ± 0.0005 g kg^{-1} yr^{-1} and –0.0007 ± 0.0005 g kg^{-1} yr^{-1}, respectively. This implied on a lightening trend of –0.0011 ± 0.0010 kg m^{-3} yr^{-1} and –0.0017 ± 0.0012 kg m^{-3} yr^{-1} for each basin, respectively. The freshening and lightening behavior found here bring an indication of a circumpolar change in the salinity and density of coastal waters around Antarctica. The lower rates of freshening and lightening compared to previous studies (e.g., Azaneu et al., 2013; Dotto et al., 2016) is caused by a salinity reversal that occurred during the period 2010-2016.

Changes in the source water fractions of the deep water mixture have been attributed to the high degree of thermohaline interannual variability found in the central and eastern basins of the Bransfield Strait. For example, from 2010 to 2016, one can observe an increased contribution of ~17% for HSSW and of 2% for CDW in the Bransfield Strait central and eastern basins, and a corresponding decrease of ~18% in LSSW. This change in the mixing ratio of source waters is suggested as responsible for the increase in salinity of deep waters observed in the central basin. On the other hand, from 2016 to 2019, there was an increase in LSSW and HSSW of ~11% and 1%, respectively, concomitant with a decrease of ~12% in CDW. This change was likely responsible for the freshening observed in the Bransfield Strait in that period.

The deep waters variability in the Bransfield Strait is linked to regional atmospheric patterns and variability, which is related to the SAM and ENSO climate modes. These modes influence (i) the intensity of the Weddell Gyre and the Antarctic Coastal Current system on the western edge of the Weddell Sea, (ii) the migration of the fronts associated with the Antarctic Circumpolar Current, as well as (iii) the regional sea ice formation, circulation and

accumulation patterns. Hence, the variability associated with those climate modes alters the pattern of Dense Shelf Water intrusion that gives rise to the deep waters of the Bransfield Strait.

The results found here seem to be associated with a recent circumpolar alteration of the hydrographic properties in the Southern Ocean. A peculiar combination of El Niño and positive SAM that likely led to higher sea ice formation in the western Weddell Sea in 2015 and 2016 contributed to the reversal of freshening observed in the Bransfield Strait during 2010-2019. Similar processes have recently been described around the Southern Ocean (e.g., Catagno et al., 2019; Aoki et al., 2020b; Silvano et al., 2020). These changes of the hydrographic properties are considerable for the interannual variability when compared to the long-term freshening observed in coastal areas. However, in our study, the salinity decreased again after this period, contributing to the known long-term freshening in the Bransfield Strait. Therefore, understanding if this will be a general pattern observed in the future and the consequences for the exported Antarctic Bottom Water seems a task for future studies. Finally, the hydrographic properties recorded on our time series, spanning through six decades across the Bransfield Strait, is much longer than those previously reported in the Weddell Sea. Thus, these longer time series provide further and stronger evidence on how climate variability affects the bottom water in the Southern Ocean.

Acknowledgements

This study is part of the activities of the Brazilian High Latitude Oceanography Group (GOAL) within the Brazilian Antarctic Program (PROANTAR). GOAL has been funded by and/or has received logistical support from the Brazilian Ministry of the Environment (MMA); the Brazilian Ministry of Science, Technology, and Innovation (MCTI); the Council for Research and Scientific Development of Brazil (CNPq); the Brazilian Navy; the Inter-ministerial Secretariat for Sea Resources (SECIRM); the National Institute of Science and Technology of the Cryosphere (INCT CRIOSFERA; CNPq grant nos. 573720/2008-8 and 465680/2014-3); and the Research Support Foundation of the State of Rio Grande do Sul (FAPERGS grant No. 17/2551-000518-0). This study was conducted within the activities of the GOAL projects (CNPq grant nos. 550370/2002-1, 520189/2006-0, 556848/2009-8, 565040/2010-3, 405869/2013-4, 407889/2013-2, 442628/2018-8 and 442637/2018-7, respectively). Financial support was also received from Coordination for the Improvement of Higher Education Personnel (CAPES) through the project CAPES "Ciências do Mar" (grant no. 23038.001421/2014-30). CAPES also provided free access to many relevant journals though the portal "Periódicos CAPES" and the activities of the Graduate Program in Oceanology. Rodrigo Kerr and Mauricio M. Mata are granted with researcher fellowships from CNPq grant nos. 304937/2018-5 and 306896/2015-0, respectively. Tiago S. Dotto acknowledges financial support from CNPq PDJ scholarship grant no. 151248/2019-2. The authors thank the officers and crew of the polar vessels *Ary Rongel* and *Almirante Maximiano* of the Brazilian Navy, and the several scientists and technicians participating in the cruises for their valuable help during data sampling and data processing. We thank all scientists and research groups for making their data available. All data sets used and respective websites are indicated in the manuscript. We are grateful for the constructive comments provided by two anonymous reviewers which substantially improved the manuscript.

References

Aoki, S., Katsumata, K., Hamaguchi, M., Noda, A., Kitade, Y., Shimada, K., et al. (2020a). Freshening of Antarctic bottom water off Cape Darnley, East Antarctica. *Journal of Geophysical Research: Oceans*, 125, e2020JC016374, https://doi.org/10.1029/2020JC016374

Aoki, S., Yamazaki, K., Hirano, D. et al. (2020b). Reversal of freshening trend of Antarctic Bottom Water in the Australian–Antarctic Basin during 2010s. *Scientific Reports*, 10, 14415, https://doi.org/10.1038/s41598–020–71290–6

Abrahamsen, E. P., Meijers, A. J. S., Polzin, K. L., Naveira Garabato, A. C., King, B. A., Firing, Y. L., et al. (2019). Stabilization of dense Antarctic water supply to the Atlantic Ocean overturning circulation. *Nature Climate Change*, *9* (10), 742–746. http://doi.org/10.1038/s41558–019–0561–2

Abernathey, R., Cerovecki, I., Holland, P. et al. (2016). Water-mass transformation by sea ice in the upper branch of the Southern Ocean overturning. *Nature Geoscience* 9, 596–601. https://doi.org/10.1038/ngeo2749

Almeida, L., Azevedo, J. L. L., Kerr, R., Araujo M., & Mata, M. M. (2018). Impact of the new equation of state of seawater (TEOS–10) on the estimates of water mass mixture and meridional transport in the Atlantic Ocean. *Progress in Oceanography*, *162*, 13–24. https://doi.org/10.1016/j.pocean.2018.02.008

Amblas, D., & Dowdeswell, J. A. *(*2018*)*. Physiographic influences on dense shelf-water cascading down the Antarctic continental slope. *Earth-Science Reviews*, 185, 887–900. https://doi.org/10.1016/j.earscirev.2018.07.014

Avelina, R., Leticia C. da Cunha, Cássia de O. Farias, Claudia Hamacher, Rodrigo Kerr, Mauricio M. Mata. (2020). Contrasting dissolved organic carbon concentrations in the Bransfield Strait, Northern Antarctic Peninsula: insights into ENSO and SAM effects, *Journal of Marine Systems*, 212, 103457. https://doi.org/10.1016/j.jmarsys.2020.103457

Azaneu, M., Kerr, R., Mata, M.M., & Garcia, C.A.E., (2013). Trends in the deep Southern Ocean (1958–2010): implications for Antarctic Bottom Water properties and volume export. *Journal Geophyscal Research: Oceans 118*, 1–15. http://dx.doi.org/10.1002/jgre.20303

Barbat, M. M., Rackow, T., Wesche, C., Hellmer, H. H., Mata, M. M., (2021). Automated iceberg tracking with a machine learning approach applied to SAR imagery: A Weddell Sea case study. Journal of Photogrammetry and Remote Sensing, 172, 189-206, https://doi.org/10.1016/j.isprsjprs.2020.12.006

Bintanja, R., van Oldenborgh, G., Drijfhout, S. et al., (2013). Important role for ocean warming and increased ice-shelf melt in Antarctic sea-ice expansion. *Nature Geoscience*, 6, 376–379. https://doi.org/10.1038/ngeo1767

Boyer, T.P., et al., (2013). World ocean database 2013. In: Levitus, S., Mishonov, A. (Eds.).(2013) *NOAA Atlas NESDIS 72*. Silver Spring, Md., pp. 209. http://dx.doi.org/10.7289/V5NZ85MT

Carmack, E. C. (1974), A quantitative characterization of water masses in the Weddell Sea during summer. *Deep Sea Research Oceanographic Abstracts*, 74, 431–443. https://doi.org/10.1016/0011–7471(74)90092–8

Carmack, E. C., & T. D. Foster (1975). On the flow of water out of the Weddell Sea. *Deep Sea Research Oceanographic Abstracts*, 22. 711–724. https://doi.org/10.1016/0011–7471(75)90077–7

Castagno, P., Capozzi, V., DiTullio, G.R. et al. (2019). Rebound of shelf water salinity in the Ross Sea. *Nature Communications*, 10, 5441, https://doi.org/10.1038/s41467–019–13083–8

Cavalieri, D. J., Gloersen, P., & Campbell, W. J. (1984). Determination of sea-ice parameters with the Nimbus-7 SMMR. *Journal of Geophysical Research*, 89 (D4), 5355–5369. https://doi.org/10.1029/JD089iD04p05355

Clem, K. R., Renwick, J. A., McGregor, J., and Fogt, R. L. (2016). The relative influence of ENSO and SAM on Antarctic Peninsula climate, Journal of Geophysical Research Atmospheric, 121, 9324– 9341, http://dx.doi.org/10.1002/2016JD025305

Collares, L. L., Mata, M.M., Kerr, R., Arigony, J., & Barbat, M. (2018). Iceberg drift and ocean circulation in the northwestern Weddell Sea, Antarctica. *Deep Sea Research Part II: Topical Studies in Oceanography, 149*, 10–24. http://doi.org/10.1016/j.dsr2.2018.02.014

Cook, A.J., Holland, P.R., Meredith, M.P., Murray, T., Luckman, A., & Vaughan, D. G. (2016). Ocean forcing of glacier retreat in the western Antarctic Peninsula. *Science*, 353: 283–286. http://dx.doi.org/10.1126/science.aae0017

Costa, R. R., Mendes, C. R. B., Tavano, V. M., Dotto, T. S., Kerr, R., Monteiro, T., et al. (2020). Dynamics of an intense diatom bloom in the Northern Antarctic Peninsula. February 2016. *Limnology Oceanography* 65, 2056–2075. http://dx.doi.org/10.1002/lno.11437

Dotto, T. S., Kerr, R., Mata, M. M., & Garcia, C. A. E. (2016). Multidecadal freshening and lightening in the deep waters of the Bransfield Strait, Antarctica. *Journal of Geophysical Research Oceans*, *121*(6), 3741–3756. https://doi.org/10.1002/2015JC011228

Dotto, T. S., Mata, M. M., Kerr, R. & Garcia, C. A. E. (2021). A novel hydrographic gridded data set for the Northern Antarctic Peninsula. *Earth System Science Data*, 671–696, https://doi.org/10.5194/essd-13-671-2021

Fahrbach, E., Peterson, R. G., Rohardt, G., Schlosser, P., & Bayer, R. (1994). Suppression of bottom water formation in the southeastern Weddell sea. *Deep–Sea Research Part I*, 41(2), 389–411. https://doi.org/10.1016/0967–0637(94)90010–8

Fahrbach, E., Hoppema, M., Rohardt, G., Schröder, M., Wisotzki, A. (2004). Decadal–scale variations of water mass properties in the deep Weddell Sea. *Ocean Dynamics.* 54, 77–91.https://doi.org/10.1007/s10236–003–0082–3

Foldvik, A, Gammelsrod, T., & Torresen, T. (1985). Circulation and water masses on the southern Weddell Sea Shelf. *Oceanology of the Antarctic Continental Shelf*, *43*, 5–20. https://doi.org/10.1029/AR043p0005

Garcia, C. A. E., & Mata, M. M. (2005). Deep and bottom water variability in the central basin of Bransfield Strait (Antarctica) over the 1980–2005 period. *CLIVAR Exchanges*, 10(4), 48–50.

Gille, S.T. (2002). Warming of the Southern Ocean since 1950s. *Science*, 295, 1275–1277. https://doi.org/10.1126/science.1065863

Gille, S.T., (2008). Decadal–scale temperature trends in the Southern Hemisphere Ocean. *Journal of Climate*, 21, 4749–4765. http://dx.doi.org/10.1175/2008JCLI2131.1

714 Gordon, A. L., & Nowlin, Jr. W. D. (1978), The basin waters of the Bransfield Strait, *Journal*
715 *of Physical Oceanography*, 8, 258–264. http://dx.doi.org/10.1175/1520–
716 0485(1978)008<0258:TBWOTB>2.0.CO;2

717 Gordon, A.L., Mensch, M., Dong, Z., Smethie Jr., W.M., & de Bettencourt, J. (2000). Deep
718 and bottom water of the Bransfield Strait eastern and Central Basins. *Journal Geophysical*
719 *Research*, 105, 11337–11346. http://dx.doi.org/10.1029/2000JC900030

720 Gordon, A. L., Huber, B., Mckee, D., & Visbeck, M., (2010). A seasonal cycle in the export
721 of bottom water from the Weddell sea. *Nature Geoscience*, 3, 551–556,
722 http://doi.org/10.1038/ngeo916

723 Gordon, A. L., Huber, B. A., & Abrahamsen, E. P. (2020). Interannual variability of the outflow
724 of Weddell Sea Bottom Water. Geophysical Research Letters, 47, e2020GL087014.
725 https://doi.org/10.1029/2020GL087014

726 Haid, V., and Timmermann, R. (2013), Simulated heat flux and sea ice production at coastal
727 polynyas in the southwestern Weddell Sea, J. Geophys. Res. Oceans, 118, 2640- 2652,
728 doi:10.1002/jgrc.20133.

729 Hellmer, H.H., Huhn, O., Gomis, D., & Timmermann, R. (2011). On the freshening of the
730 northwestern Weddell Sea continental shelf. *Ocean Science*, 7, 305–316.
731 http://dx.doi.org/10.5194/os–7–305–2011

732 Hersbach, H., Bell, B., Berrisford, P., et al. (2020). The ERAS5 Global Reanalysis. *Quarterly*
733 *Journal of the Royal Meteorological Society*, 146, 1999– 2049.
734 https://doi.org/10.1002/qj.3803

735 Heywood, K. J., et al. (2014). Ocean processes at the Antarctic continental slope. *Philosophical*
736 *Transactions of The Royal Society A Mathematical Physical and Engineering Sciences*, 372,
737 20130047. http://dx.doi.org/10.1098/rsta.2013.0047

738 Heuzé, C., Heywood, K. J., Stevens, D. P. & Ridley, J. K. (2013). Southern Ocean Bottom
739 Water Characteristics in CMIP5 models. **G***eophysical Research Letters***,** 40(7),1 409–1414.
740 http://dx.doi.org/10.1002/grl.50287

741 Hattermann, T., Nicholls, K.W., Hellmer, H.H. et al. Observed interannual changes beneath
742 Filchner-Ronne Ice Shelf linked to large-scale atmospheric circulation. Nat Commun 12,
743 2961 (2021). https://doi.org/10.1038/s41467-021-23131-x

744 Hofmann, E.E., Klinck, J.M., Lascara, C.M., Smith, D.A. (1996). Water mass distribution and
745 circulation west of the Antarctic Peninsula and including Bransfield Strait. In: Ross, R.M.,
746 Hofmann, E.E., Quetin, L.B. (Eds.), *Antarctic Research Series*, 70, 61–80
747 http://dx.doi.org/10.1029/AR070p0061

748 Holland, P. R. (2014). The seasonality of Antarctic Sea ice trends. *Geophysical Research*
749 *Letters* 41, 4230–4237.

750 Hutchinson, K., Deshayes, J., Sallee, J.-B., Dowdeswell, J. A., de Lavergne, C., Ansorge, I., et
751 al. (2020). Water mass characteristics and distribution adjacent to Larsen C Ice Shelf,
752 Antarctica. Journal of Geophysical Research: Oceans, 125, e2019JC015855.
753 https://doi.org/10.1029/2019JC015855

754 Huhn, O., Hellmer, H. H., Rhein, M., Rodehacke, C., Roether, W., Schodlok, M., & Schr€oder,
755 M. (2008). Evidence of deep– and bottom–water for– mation in the western Weddell Sea.
756 *Deep Sea Research Part II: Topical Studies in Oceanography*, 55(8), 1098–1116.
757 http://dx.doi.org/10.1016/j.dsr2.2007.12.015

Huneke, W.G.C., Huhn, O. & Schröeder, M. (2016). Water masses in the Bransfield Strait and adjacent seas, austral summer 2013. *Polar Biology*, 39, 789–798.

Ito, R. G., Tavano, V.M., Mendes, C. R. B., Garcia, C. A. E. (2018). Sea-air CO2 fluxes and pCO2 variability in the Northern Antarctic Peninsula during three summer periods (2008–2010). *Deep-Sea Research Part II: Topical Studies in Oceanography (2018)*, 84-98, http://doi.org/10.1016/j.dsr2.2017.09.004

Jackett, D. R., & McDougall, T. J. (1997). A neutral density variable for the world's oceans. *Journal Physical Oceanographic,* 27, 237–263. http://dx.doi.org/10.1175/1520–0485(1997)0272.0.CO;2

Jacobs, S. S., C. F. Giulivi, and P. A. Mele. (2002). Freshening of the Ross Sea during the late 20th century. Science, 297, 386–389, https://doi.org/10.1126/science.1069574

Jacobs, S. S., & Giulivi, C. F. (2010). Large multidecadal salinity trends near the Pacific–Antarctic continental margin, *Journal of Climate*, 23, 4508–4524. http://dx.doi.org/10.1175/2010JCLI3284.1

Johnson, D. R., T. P. Boyer, H. E. Garcia, R. A. Locarnini, O. K. Baranova, & Zweng, M. M. (2013). World Ocean Database 2013 User's Manual, edited by S. Levitus and A. Mishonov, NODC Int. Rep. 22, NOAA Print. Off., Silver Spring, Md., 172 pp. [Available at http://www.nodc. noaa.gov/OC5/WOD13/docwod13.html.

Janout, M. A., Hellmer, H. H., Hattermann, T., Huhn, O., Sültenfuss, J., sterhus, S., et al. (2021). FRIS revisited in 2018: On the circulation and water masses at the Filchner and Ronne ice shelves in the southern Weddell Sea. Journal of Geophysical Research: Oceans, 126, e2021JC017269. https://doi.org/10.1029/2021JC017269

Jullion, L., Jones, S. C., Naveira Garabato, A. C., & Meredith, M. P. (2010). Wind–controlled export of Antarctic bottom water from the Weddell Sea, *Geophysical Research Letters*, 37, L09609. http://dx.doi.org/10.1029/2010GL042822

Jullion, L., Naveira Garabato, A. C., Meredith, M., Holland, P., Courtois, P., & King, B. (2013). Decadal freshening of the Antarctic bottom water exported from the Weddell Sea, *Journal of Climate*, 26, 8111–8125. http://dx.doi.org/10.1175/JCLI–D–12–00765.1

Kerr, R., Mata, M. M., & Garcia, C. A. E. (2009). On the temporal variability of the Weddell Sea Deep water masses, *Antarctic Science*, 21(4), 383–400. http://dx.doi.org/10.1017/S0954102009001990

Kerr, R., Heywood, K.J., Mata, M.M., & Garcia, C.A.E. (2012). On the outflow of dense water from the Weddell and Ross Sea in OCCAM model. *Ocean Science*, 8, 369–388. http://dx.doi.org/10.5194/os–8–369–2012

Kerr, R., Mata, M. M., Mendes, C. R. B., & Secchi, E. R. (2018a). Northern Antarctic Peninsula: a marine climate hotspot of rapid changes on ecosystems and ocean dynamics. *Deep Sea Research Part II Topical Studies in Oceanography*. 149, 4–9. http://dx.doi.org/10.1016/j.dsr2.2018.05.006

Kerr, R., Dotto, T. S., Mata, M. M. & Hellmer, H. H. (2018b). Three decades of deep water mass investigation in the Weddell Sea (1984–2014): Temporal variability and changes. *Deep Sea Research Part II: Topical Studies in Oceanography*, 149, 70–83. http://dx.doi.org/10.1016/j.dsr2.2017.12.002

Kumar, A., Yadav, J., and Mohan, R. (2021). Seasonal sea-ice variability and its trend in the Weddell Sea sector of West Antarctica. *Environmental Research Letters*. 16 024046. https://doi.org/10.1088/1748-9326/abdc88

Kusahara, K., & Hasumi H. (2014). Pathways of basal meltwater from Antarctic ice shelves: A model study. *Journal Geophysical Research: Oceans,* 119, 5690–5704. http://dx.doi.org/10.1002/2014JC009915

Lago, V., & England, M. H. (2019). Projected Slowdown of Antarctic Bottom Water Formation in Response to Amplified Meltwater Contributions. *Journal of Climate*, 32(19), 6319-6335. Retrieved Dec 27, 2020, from https://journals.ametsoc.org/view/journals/clim/32/19/jcli-d-18-0622.1.xml

Leffanue, H., & Tomczak, M. (2004). Using OMP analysis to observe temporal variability in water mass distribution, *Journal Marine Research,* 48, 3–14. http://dx.doi.org/10.1016/j.jmarsys.2003.07.004

Lin, X., Zhai, X., Wang, Z. & Munday, D., (2018). Mean, variability and trend of Southern Ocean wind stress: Role of wind fluctuations. *Journal of Climate,* 31(9), 3557–3573. https://doi.org/10.1175/JCLI–D–17–0481.1

Liu, J.P., J.A. Curry, and Y. Hu, (2004). Recent Arctic sea-ice variability: Connections to the Arctic Oscillation and the ENSO. *Geophysical Research Letters*, 31, L09211, http://dx.doi.org/10.1029/2004GL019858

Loeb, V.J., Hofmann, E.E., Klinck, J.M., Holm–Hansen, O., White, W.B., (2009). ENSO andvariability of the Antarctic Peninsula pelagic marine ecosystem. *Antarctic Science* 21 (2),135–148. http://dx.doi.org/10.1017/S0954102008001636

Loeb, V. J., Hofmann, E. E., Klinck, J. M., & Holm–Hansen, O. (2010). Hydrographic control of the marine ecosystem in the South Shetland Elephant Island and Bransfield Strait region. *Deep Sea Research Part II: Topical Studies in Oceanography*, *57*, 519–542. https://doi.org/10.1016/j.dsr2.2009.10.004

López, O., Garcia, M. A., Gomis, D., Rojas, P., Sospedra, J., & Arcilla. (1999). Hydrographic and hydrodynamic characteristics aof the eastern basin of the Bransfiled Strait. *Deep Sea Research Part I: Oceanographic Research Papers*, 46(10), 1755–1778. https://doi.org/10.1016/S0967–0637(99)00017–5

Marshall, G. (2003). Trends in the Southern annular mode from observations and reanalyses. *Journal of Climate*, 16(24), 4134–4143 https://doi.org/10.1175/1520–0442(2003)016<4134:TITSAM>2.0.CO;2

Marshall, G.J., Stott, P.A., Turner, J., Connolley, W.M., King, J.C., & Lachlan–Cope, T.A. (2004). Causes of exceptional atmospheric circulation changes in the Southern Hemisphere. *Geophysical Research Letters,* 31, L14205. http://dx.doi.org/10.1029/2004GL019952

Marshall, G.J., Orr, A., van Lipzig, N.P.M., & King, J.C. (2006). The impact of a changing Southern Hemisphere Annular Mode on Antarctic Peninsula summer temperatures. *Journal of Climate*, 19, 5388–5404.

Mata, M. M., Tavano, V. M., & Garcia, C. A. E. (2018). 15 years sailing with the Brazilian High Latitude Oceanography Group (GOAL). *Deep Sea Research Part II: Topical Studies in Oceanography*, 149, 1–3. https://doi.org/10.1016/j.dsr2.2018.05.007.

McDougall, T.J. & Barker, P.M. (2011). Getting started with TEOS–10 and the Gibbs Seawater (GSW) Oceanographic Toolbox, 28. SCOR/IAPSO WG127, ISBN 978–0–646–55621–5.

McKee, D.C., Yuan, X., Gordon, A.L., Huber, B.A., & Dong, Z. (2011). Climatic impact on interannual variability of Weddell Sea Bottom Water. *Journal Geophysical Research,* 116, C05020. http://dx.doi.org/10.1029/2010JC006484

Meehl, G.A., Arblaster, J.M., Chung, C.T.Y. et al. (2016). Sustained ocean changes contributed to sudden Antarctic sea ice retreat in late. *Nature Communications* 10, 14 (2019). https://doi.org/10.1038/s41467-018-07865-9

Meijers, A. J. S., Cerovečki, I., King, B. A., & Tamsitt, V. (2019). A see-saw in Pacific Subantarctic Mode Water formation driven by atmospheric modes. *Geophysical Research Letters*, 46, 13152– 13160, https://doi.org/10.1029/2019GL085280

Merino, N., N. C. Jourdain, J. Le Sommer, H. Goosse, P. Mathiot, and G. Durand. (2018). Impact of increasing Antarctic glacial freshwater release on regional sea-ice cover in the Southern Ocean. Ocean Modell., 121, 76–89, https://doi.org/10.1016/j.ocemod.2017.11.009

Moffat, C., and Meredith, M. P. (2018). Shelf–ocean exchange and hydrography west of the Antarctic Peninsula: a review. *Philosophical Transactions of the Royal Society A* 376:20170164. http://dx.doi.org/10.1098/rsta.2017.0164

Nicholls, K.W., Østerhus, B., Makinson, K., Gammelsrod, T., Fahrbach, E. (2009). Ice–ocean processes over the continental shelf of the southern Weddell Sea, Antarctica. A review, *Reviews of Geophysics,* 47, RG3003. http://dx.doi.org/10.1029/2007/RG000250

Niiler, P.P., Amos, A., Hu, J.–H. (1991). Water masses and 200 m relative geostrophic circulation in the western Bransfield Strait region. *Deep Sea Research, Part I,* 38, 943–959. http://dx.doi.org/10.1016/0198–0149(91)90091–S

Orsi, A.H., Whitworth, T., Nowlin Jr., W.D. (1995). On the meridional extent and fronts of the Antarctic Circumpolar Current. *Deep Sea Research Part I: Oceanographic Research Papers,* 42, 641–673. http://dx.doi.org/10.1016/0967–0637(95)00021–W

Paolo, S. F., Fricker, A. H., & Padman, L. (2015). Volume loss from Antarctic ice shelves is accelerating. *Science,* 348(6232), 327–331, http://dx.doi.org/10.1126/science.aaa0940

Purkey, S. G., and Johnson, G. C. (2012). Global Contraction of Antarctic Bottom Water between the 1980s and 2000s. *Journal of Climate* 25, 17, 5830-5844, https://doi.org/10.1175/JCLI-D-11-00612.1

Purkey, S. G., and Johnson, G. C. (2013). Antarctic bottom water warming and freshening: Contributions to sea level rise, ocean freshwater budgets, and global heat gain, *Journal of Climate,* 26, 6105–6122. http://dx.doi.org/10.1175/JCLI–D–12–00834.1

Renner, A.H.H., Thorpe, S.E., Heywood, K.J., Murphy, E.J., Watkins, J.L., Meredith, M.P. (2012). Advective pathways near the tip of the Antarctic Peninsula: trends, variability and ecosystem implications. *Deep Sea Research Part I: Oceanographic Research Papers,* 63, 91–101. http://dx.doi.org/10.1016/j.dsr.2012.01.009

Rignot, E., Mouginot, J., Scheuchl, B., van den Broeke, M., van Wessem, M. J., Morlighem, M. (2019). Four decades of Antarctic Ice Sheet mass balance from 1979–2017, *Proceedings of National Academy of Sciences of the United States of America,* 116 (4) 1095–1103. https://doi.org/10.1073/pnas.1812883116

Rintoul, S. R. (2007). Rapid freshening of Antarctic Bottom Water formed in the Indian and Pacific oceans,Geophys. Research Letters, 34, L06606, http://doi.org/10.1029/2006GL028550l

Ruiz Barlett, E. M., Piola, A. R., Mata, M. M., Tosonotto, G. V., and Sierra, M. E. (2018). On the temporal variability of intermediate and deep waters in the Western Basin of the Bransfield Strait. *Deep Sea Research Part II: Topical Studies in Oceanography*, *149*(1), 31–46. https://doi.org/10.1016/j.dsr2.2017.12.010

Sangrà, P., Gordo, C., Hernández–Arencibia, M., Marrero–Díaz, A., Rodríguez–Santana, A., Stegner, A., Martínez–Marrero, A., Pelegrí, J.L., Pichon, T. (2011). Bransfield Curr. Syst. *Deep Sea Research Part I: Oceanographic Research Papers*, 58, 390–402. http://dx.doi.org/10.1016/j.dsr.2011.01.011

Sangrà, P., Stegner, A., Hernández–Arencibia, M., Marrero–Díaz, A., Salinas, C., Aguiar–González, B., Henríquez–Pastene, C. (2017). The Bransfield gravity current. *Deep Sea Research Part I: Oceanographic Research Papers* 119, 1–15. http://dx.doi.org/10.1016/j.dsr.2016.11.003

Schmidtko, S., Heywood, K.J., Thompson, A.F., Aoki, S. (2014). Multidecadal warming of Antarctic waters. *Science* 346, 1227–1231. http://dx.doi.org/10.1126/science.1256117

Shepherd, A.,et al. *(*2018*).* Mass balance of the Antarctic Ice Sheet from 1992 to 2017. *Nature*, *558*, 219–222. https://doi.org/10.1038/s41586-018-0179-y

Sian F. Henley, Oscar M. Schofield, Katharine R. Hendry, Irene R. Schloss, Deborah K. Steinberg, Carlos Moffat, Lloyd S. Peck, Daniel P. Costa, Dorothee C.E. Bakker, Claire Hughes, Patrick D. Rozema, Hugh W. Ducklow, Doris Abele, Jacqueline Stefels, Maria A. Van Leeuwe, Corina P.D. Brussaard, Anita G.J. Buma, Josh Kohut, Ricardo Sahade, Ari S. Friedlaender, Sharon E. Stammerjohn, Hugh J. Venables, Michael P. Meredith. (2019). Variability and change in the west Antarctic Peninsula marine system: Research priorities and opportunities. *Progress in oceanography,* 173, 208-237. https://doi.org/10.1016/j.pocean.2019.03.003

Silvano, A., Rintoul, S. R., Peña-Molino, B., Hobbs, W. R., van Wijk, E., Aoki, S., Tamura, T., Williams, G. D. (2018). Freshening by glacial meltwater enhances melting of ice shelves and reduces formation of Antarctic Bottom Water. *Science Adv*ances, 4, eaap9467.

Silvano, A.; Foppert, A.; Rintoul, S.R.; Holland, P.R.; Tamura, T.; Kimura, N.; Castagno, P.; Falco, P.; Budillon, G.; Haumann, F.A., et al. (2020). Recent recovery of Antarctic Bottom Water formation in the Ross Sea driven by climate anomalies. *Nature Geoscience*, 13, 780–786

Spence, P., Griffies, S. M., England, M. H., Hogg, A. McC., Saenko, O. A., & Jourdain, N. C. (2014), Rapid subsurface warming and circulation changes of Antarctic coastal waters by poleward shifting winds. *Geophysical Research Letters*, 41, 4601–4610 http://dx.doi.org/10.1002/2014GL06061

Smith, C.A. and Sardeshmukh, P.D. (2000), The effect of ENSO on the intraseasonal variance of surface temperatures in winter. Int. J. Climatol., 20: 1543-1557. https://doi.org/10.1002/1097-0088(20001115)20:13<1543::AID-JOC579>3.0.CO;2-A

Stammerjohn, S.E., Martinson, D.G., Smith, R.C., Yuan, X. (2008). Trends in Antarcticannual sea-ice retreat and advance and their relation to El Niño–Southern Oscillationand Southern Annular Mode. *Journal of Geophysical Research*, 113, C03S90. http://dx.doi.org/10.1029/2007JC004269

Tamura, T., K. I. Ohshima, S. Nihashi, and H. Hasumi. (2011): Estimation of surface heat/salt fluxes associated with sea ice growth/melt in the Southern Ocean. SOLA, 7, 17–20, http://dx.doi.org/10.2151/sola.2011-005

Thompson, A. F., Heywood, K. J., Thorpe, S. E., Renner, A. H. H., & Trasvina, A. (2009). Surface circulation at the tip of the Antarctic Peninsula from drifters, *Journal Physics in Oceanographic*, 39, 3–26. http://dx.doi.org/10.1175/2008JPO3995.1

Timmerman, R., Hellmer, H.H., Beckmann, A. (2002). Simulations of ice–ocean dynamics in the Weddell Sea Part II: interannual variability 1985–1993. *Journal Geophysical Research*, 107. http://dx.doi.org/101029/2000JC00742

Tomczak, M., & Large, D. G. B. (1989), Optimum multiparameter analysis of mixing in the thermocline of the eastern Indian Ocean, *Journal Geophysical Research*, 94(C11), 16,141–16,149. http://dx.doi.org/10.1029/JC094iC11p16141

Tomczak, M., & Liefrink, S. (2005), Interannual variations of water mass volumes in the Southern Ocean, J. Atmos. *Ocean Science*, 10(1), 31–42. http://dx.doi.org/10.1080/17417530500062838

Turner, J., Barrand, N., Bracegirdle, T., Convey, P., Hodgson, D., Jarvis, M., Klepikov, A. (2013). Antarctic climate change and the environment: An update. *Polar Record*, 50(3), 237–259. http://dx.doi.org/10.1017/S0032247413000296

Turner, J., Guarino, M. V., Arnatt, J., Jena, B., Marshall, G. J., Phillips, T., et al. (2020). Recent decrease of summer sea ice in the Weddell Sea, Antarctica. Geophysical Research Letters, 47, e2020GL087127. https://doi.org/10.1029/2020GL087127

Van Caspel, M., Schröeder, M., Huhn, O., & Hellmer, H.H. (2015). Precursors of Antarctic bottom water formed on the continental shelf off Larsen ice shelf. *Deep Sea Research Part I:Oceanographic Research Papers*, 99, 1–9. http://dx.doi.org/10.1016/j.dsr.2015.01.004

Van Caspel, M., Hellmer, H.H., & Mata, M.M. (2018). On the ventilation of Bransfield Strait deep basins. *Deep Sea Research Part II: Topical Studies in Oceanography, 149, 25–30.* https://doi.org/10.1016/j.dsr2.2017.09.006

van den Broeke, M. (2005). Strong surface melting preceded collapse of Antarctic Peninsula ice shelf. *Geophysical Research Letters*, *32*(12), 1–4. https://doi.org/10.1029/2005GL023247

van Wijk, E. M., & Rintoul, S. R. (2014). Freshening drives contraction of Antarctic bottom water in the Australian Antarctic basin, *Geophysical Research. Letters*, 41, 1657–1664. http://dx.doi.org/10.1002/2013GL058921

Venegas, S. A. and Drinkwater, M. R. (2001). Sea ice, atmosphere and upper ocean variability in the Weddell Sea, Antarctica *Journal Geophysical Research*, 106 16747–65.

Von Gyldenfeldt, A. B., Fahrbach, E., García, M.A., Shröder, M. (2002). Flow variability at the tip of the Antarctic Peninsula. *Deep Sea Research, Part II: Topical Studies in Oceanography*, 49, 4743–4766. http://dx.doi.org/10.1016/S0967–0645(02)00157–1

Wilson, C., Klinkhammer, G. P., & Chin, C. S. (1999). Hydrography within the central and east basins of the Bransfield Strait, Antarctica. *Journal of Physical Oceanography*, 29(3), 465–479. http://dx.doi.org/10.1175/1520–0485(1999)029<0465:HWTCAE>2.0.CO;2

Williams, G., Herraiz-Borreguero, L., Roquet, F. et al. (2016) The suppression of Antarctic bottom water formation by melting ice shelves in Prydz Bay. *Nature Communications*, 7, 12577. https://doi.org/10.1038/ncomms12577

Yuan, X., (2004). ENSO–related impacts on Antarctic sea-ice: a synthesis of phenomenon and mechanisms. *Antarctic Science*, 16, 415–425. https://doi.org/10.1017/S0954102004002238

Yuan, X., Kaplan, M. R., & Cane, M. A. (2018). The interconnected global climate system—A review of tropical–polar teleconnections. *Journal of Climate*, 31(15), 5765–5792. https://doi.org/10.1175/JCLI–D–16–0637.1

Youngs, M. K., Thompson, A. F., Flexas, M. M., & Heywood, K. J. (2015) Weddell sea export pathways from surface drifters, J*Journal of Physical Oceanography*, 45, 1068–1085. http://dx.doi.org/10.1175/JPO–D–14–0103.1

Zhou, M., Niiler, P.P., Hu, J.–H. (2002). Surface currents in the Bransfield and Gerlache Straits, Antarctica. *Deep Sea Research Part I:Oceanographic Research Papers*, 49 (2), 267–280. http://dx.doi.org/10.1016/S0967–0637(01)00062–0

Zhou, M., Niiler, P.P., Zhu, Y., Dorly, R.D. (2006). The western boundary current in the Bransfield Strait, Antarctica. *Deep Sea Research Part I:Oceanographic Research Papers*, 53, 1244–1252. http://dx.doi.org/10.1016/j.dsr.2006.04.003

Zhou, Q., Hattermann, T., Nøst, O. A., Biuw, M., Kovacs, K. M., and Lydersen, C. (2014), Wind-driven spreading of fresh surface water beneath ice shelves in the Eastern Weddell Sea, *Journal of Geophysical Research: Oceans*, 119, 3818– 3833, http://dx.doi.org/10.1002/2013JC009556

Highlights:

- Long–term cooling, freshening, and lightening (1963-2019) of deep waters in the Bransfield central basin.
- Decreasing ventilation in the Bransfield Strait eastern basin as oxygen declined.
- Reversal of freshening trend between 2010 and 2016 associated with increased contribution of High Salinity Shelf Water.
- Decreasing in salinity after 2016 caused by increased contribution of Low Salinity Shelf Water.
- Increased contribution of High Salinity Shelf Water in the Bransfield Strait related to increased sea ice cover in the northwestern Weddell Sea.

Declaration of interests

☒ The authors declare that they have no known competing financial interests or personal relationships that could have appeared to influence the work reported in this paper.

☐The authors declare the following financial interests/personal relationships which may be considered as potential competing interests.